

SEIB–DGVM v2.10 online description document (Last modified: 22 April 2008)

Written by Hisashi SATO (FRCGC-JAMSTEC)

Note: In this major update, we improved SEIB-DGVM for reconstructing vegetation dynamics in Boreal needle-leaved summer green forest and Tropical rain forest. By now, the paper for former research is submitted, while the latter study is in preparation. Thus, we only describe modifications conducted for Boreal needle-leaved summer green forest. When we submitted the latter study, we will describe modifications conducted for Tropical rain forest.

Overview

The simulation unit of the SEIB–DGVM is a 30×30 -m spatially explicit virtual forest, in which individual trees establish, compete, and die. A grass layer also exists in the forest under the tree canopy. Appendix B1 shows the input and output of the model. Appendix B2 summarizes the processes represented, which can be classified into three groups: physical, physiological, and vegetation dynamics. The SEIB–DGVM utilizes three computational time steps: a daily time step for all physical and physiological processes except for soil decomposition and tree growth, a monthly time step for soil decomposition and tree growth, and an annual time step for vegetation dynamics and disturbance. Appendix B3 lists the symbols used in the model's equations. Those that begin with a capital letter are constants, while those that begin with a lowercase letter are variables. Plant species are classified into small number of plant functional types (PFTs) to enable global-scale simulation (Table 1). These PFTs can coexist in the same simulation plot.

Plant properties

Woody PFTs are represented by individual trees composed of three organs: the crown and the trunk, both of which are cylindrical, and the fine roots, which are formless (Fig. 1). The crown is defined by biomass ($mass_{leaf}$), leaf area (la), diameter ($crown_{diameter}$), and depth ($crown_{depth}$); the trunk, by biomass ($mass_{trunk}$), height ($height$), and the diameters of sapwood ($dbh_{sapwood}$) and heartwood ($dbh_{heartwood}$); the fine roots, by biomass ($mass_{root}$) only. Trunk biomass ($mass_{trunk}$) includes both branch and coarse root biomass. Besides these variables, each individual tree has a reserve resource ($mass_{stock}$), which is used for foliation after the dormant phase (for deciduous PFTs) and after fires. Grass PFTs are represented in a much simpler way, consisting of leaf, root, and a reserve resource, all of which are represented by biomass per unit area ($gmass_{leaf}$, $gmass_{root}$, and $gmass_{stock}$, respectively).

Carbon cycles

Figure 2 provides an overview of the carbon cycle as represented in the SEIB-DGVM. Atmospheric CO_2 is assimilated by the foliage of woody PFTs and grass PFTs. This assimilated carbon is then transferred to all of the other organs, where maintenance and growth respiration occurs. All respired carbon is recycled to the atmosphere as CO_2 . At the same time, defoliation at the end of the growing season, turnover of leaves and fine roots, and tree death produce litter, which is added to the litter pool. When the litter pool decomposes, some portion of the carbon within it is recycled to the atmosphere, while the remaining carbon is added to pools of soil organic carbon 1 (fast decomposition rate) or 2 (slow decomposition rate). Finally, decomposed soil organic carbon is recycled to the atmosphere as CO_2 .

Water cycles

Figure 3 provides an overview of the water cycle as represented in the model. The ground is composed of three soil layers: soil layer 1, soil layer 2, and soil layer 3. Depth of each soil layer, $Depth_{(1)}$, $Depth_{(2)}$, $Depth_{(3)}$, is 500 mm, 1000 mm, and 1500 mm, respectively. Hydrological and radiation properties of soil is given by 5 grid-specific parameters, $ALBEDO$, W_{sat} , W_{fi} , W_{mat} , and W_{wilt} . Each parameter indicates soil albedo, soil moisture at saturation point, field capacity, matrix potential, and wilting point, respectively. Water can be pooled as snow ($pool_{snow}$) and as water in soil layers 1, 2, and 3 ($pool_{w(1)}$, $pool_{w(2)}$, and $pool_{w(3)}$, respectively). Percolated water from soil layer 3 is immediately removed as runoff.

Daily water flow (in the order of computation)

Precipitation ($prec$) is divided into rainfall ($prec_{rain}$) and snowfall ($prec_{snow}$) using empirical function of the daily mean temperature of air (tmp_{air}) (Ito and Oikawa, 2002):

$$prec_{snow} = prec / [1 + \exp(0.75 \times tmp_{air} - 1.5)] \quad (1)$$

$$prec_{rain} = prec - prec_{snow}. \quad (2)$$

Snowfall is added to the snow pool ($pool_{snow}$), which melts as a function of soil temperature (tmp_{soil}):

$$\Delta pool_{snow} = prec_{snow} - tw \quad (3)$$

$$tw = pool_{snow} / [1 + \exp(-0.3 (tmp_{soil} - 10))], \quad (4)$$

where tw is daily snow melting water. A portion of the rainfall is caught by leaves, and evaporates before reaching the soil surface. The fraction of this intercepted rainfall is a function of leaf area index (lai in $m^2 m^{-2}$).

$$ic = \min [prec_{rain}, 3.0 \times rain \times (1.0 - \exp(-1.0 \times lai))], \quad (5)$$

where $rain$ is expected number of rain in a day, which is calculated using method in Neilson(1992). From the above equations, the daily liquid water to reach the soil surface can be calculated as $prec_{rain} + tw - ic$. Some of this water $pn_{(0)}$ infiltrates soil layer 1, while the rest $(prec_{rain} + tw - ic) - pn_{(0)}$ washes off the surface as runoff (see Appendix A5 for calculation of $pn_{(0)}$).

Daily changes of the soil water storages (in the order of computation)

The daily changes in soil water storage are represented as follows, where ev , $tr_{(n)}$, and $pn_{(n)}$ are the rates of evaporation from soil surface, transpiration from soil layer n , and penetration from soil layer n , respectively:

$$\Delta pool_{w(1)} = (pn_{(0)} - pn_{(1)}) - tr_{(1)} - ev \quad (6)$$

$$\Delta pool_{w(2)} = (pn_{(1)} - pn_{(2)}) - tr_{(2)} \quad (7)$$

$$\Delta pool_{w(3)} = (pn_{(2)} - pn_{(3)}). \quad (8)$$

This model neglects the upward movement of capillary water under dry conditions. The

computational methods for penetration and evapotranspiration are detailed in Appendix A5 and A6, respectively.

To control leaf phenology and the rate of photosynthesis as a function of soil water availability, the physiological status of water availability is defined for each PFT ($stat_{water}$, 0.0–1.0) as follows:

$$stat_{water} = \frac{\max\left(\frac{pool_{w(1)}}{Depth_{(1)}}, \frac{pool_{w(2)}}{Depth_{(2)}}\right) - W_{wilt}}{W_{fi} - W_{wilt}} . \quad (9)$$

When soil temperature is less than 0 °C, $stat_{water}$ is assumed to be zero.

Establishment of Woody PFTs

In the model, new individual trees establish on the last day of each simulation year. It is assumed that establishment only occurs if total precipitation of the current year (in mm) exceeds 20 times the annual mean temperature (in °C) (Köppen, 1936). Each woody PFT has distinct of climatic range for establishment, following the LPJ–DGVM (Sitch et al., 2003): the maximum coldest-month temperature (TC_{max}), and the minimum growing-degree day (GDD_{min}), as shown in Appendix B5. Both climatic limitations are applied to the running means of the last 20 years. For some PFTs, we assumed that they can only establish when the midday photosynthetically active radiation (PAR, hereafter) that averaged for the previous year exceeded PAR_{min} $\mu\text{mol photon m}^{-2} \text{ s}^{-1}$ at the surface of the grass layer. For some PFTs, we additionally assumed that they cannot establish when drought month (monthly means of $stat_{water} < 0.3$) continued more than DM_{max} month in the previous year.

All newly established trees have 0.01 m of $dbh_{sapwood}$, 0.00 m of $dbh_{heartwood}$, and 0 m of lowest-branch height (i.e., $height = crown_{depth}$). From these properties, tree height ($height$), crown diameter ($crown_{diameter}$), and stem biomass ($mass_{trunk}$) are calculated using allometric and allocation formulas described in the section titled 'tree growth.' These newly established trees initially lack leaves and fine roots, but have 500 g DM of reserve resource ($mass_{stock}$). The biomass of newly established trees is taken from the litter pool of the same forest so that total carbon storage of the forest remains the same.

The floor of the virtual forest is divided into a grid of 1.0×1.0 -m mesh, and each tree monopolizes one of the mesh boxes. The SEIB-DGVM assumes that crowns of different trees cannot occupy the same space, and thus mesh boxes in which a newly established tree interacts with existing trees are not available for further establishment. For each available mesh box, the same establishment rate, $P_{establish}$, was assumed.

There are 4 scenarios to allocate available mesh box to woody PFT that can establish under the given climate. Note, for specifying establishment scenario, specify $Est_scenario$ in the parameter file.

Scenario 1 (one specific PFT establish): only one woody PFT, which is specified by Est_pft_OnOff in the parameter file, can monopolize available mesh box.

Scenario 2 (infinite seed dispersal): every woody PFTs that can establish at the given climatic conditions share available mesh box equally.

Scenario 3 (no seed dispersal): Same as scenario 2 until specific year *Est_year_change* in the parameter file. After that, allocate available mesh box among each woody PFTs in proportion to existing biomass at the forest stand.

Scenario 4 (Scenario 3 + long dispersal seed): Same as scenario 2 until year *Est_year_change*. After that, some fraction *Est_frac_random* of available mesh box was randomly selected from all woody PFTs that can establish at the given climatic conditions, while remaining mesh boxes are allocated in proportion to existing biomass of each woody PFT.

Establishment of Grass PFTs

For grass PFTs, establishment processes are not treated explicitly. A small amount of grass 'seed' is always assumed to be present, even if the environment is unfavorable to grass survival; densities of grass biomass ($gmass_{leaf}$, $gmass_{root}$, and $gmass_{stock}$) never decrease below their minimum limits (0.1 g m^{-2} for all).

The floor of the virtual forest is disproportionately divided into two sections (90% and 10%), and each section is monopolized by one of the two grass PFTs, namely C_3 and C_4 grass. Thus, the two grass PFTs always coexist in the forest, but one dominates the other, the dominant PFT being distributed throughout the larger fraction. Dominant grass PFT was determined on the last day of each year; the grass PFT that has a higher annual NPP per unit area in the previous year will be dominant in the following year. When the dominant PFT changes, the biomass properties ($gmass_{leaf}$, $gmass_{root}$, and $gmass_{stock}$) of the two grass PFTs are exchanged so that the total grass biomass of the plot remains the same.

PAR Allocation

For each simulation day, the radiation module of the SEIB–DGVM calculates direct and diffuse components of photosynthetically active radiation at midday (par_{direct} and $par_{diffuse}$, respectively) (see Appendix A2 for the calculation). How these PARs are distributed among trees and grass primarily controls plant growth and competition.

Woody PFTs

Each tree crown is horizontally sliced into 10-cm-deep 'disks,' for which photosynthesis is calculated separately (Fig. 1). The midday PAR that enters disk l of individual n , $par_{wood(l,n)}$, is calculated as follows, where $fpar_{direct(l,n)}$ and $fpar_{diffuse(l)}$ represent the relative intensity of direct and diffuse PAR of disk l of tree n at midday compared to the forest top, respectively:

$$par_{wood(l,n)} = fpar_{direct(l,n)} \times par_{direct} + fpar_{diffuse(l)} \times par_{diffuse}. \quad (10)$$

To obtain $fpar_{direct(l,n)}$, a virtual cylinder with a cross section equal to disk l , was extended from the disk to the direction of the south with angle $0.86 \times sl_{hgt}$, where sl_{hgt} is midday solar angle (Fig. 4). The horizontal line of $0.86 \times sl_{hgt}$ equally divides daily sum of solar radiation into two, when daily changes of solar angle and solar radiation are \sin and \sin^2 , respectively. Then, the total leaf area falling within the cylinder, $fpar_{direct(l,n)}$, was summed using Beer's law as follows, where $la_{(p)}$ (m^2) is the sum of the leaf area of PFT p within the cylinder, $crown_{area(n)}$ is the cross section of the crown area of tree n , and $EK_{(p)}$ is the vertical light attenuation coefficient of PFT p :

$$fpar_{direct(l,n)} = \exp\left(\frac{-1.0 \times \sum_{p=1}^{woody-pft} (EK_{(p)} \times lai_{(p)})}{crown_{area(n)}}\right). \quad (11)$$

In this calculation, the virtual forest was assumed to repeat; i.e., if the cylinder exited the forest edge at a lower position than the tallest tree, the cylinder would reenter the forest from the opposite edge at the same position in a west–east vertical plane. The calculation of $fpar_{direct(l,n)}$ is the most computationally power-consuming process in the model. Thus, this factor is updated in five-day intervals.

Because diffuse PAR scatters in the sky, we ignored horizontal structures in the forest while calculating its distribution in the forest; all disks at the same height receive the same intensity of diffuse PAR. The relative intensity of diffuse PAR on the disk layer l , $fpar_{diffuse(l)}$, is calculated every day as follows, where $lai_{(l,p)}$ is the leaf area index ($m^2 m^{-2}$), which is calculated only for PFT p and for leaves above disk layer l :

$$fpar_{diffuse(l)} = \exp\left(-1.0 \times \sum_{p=1}^{woody-pft} (EK_{(p)} \times lai_{(l,p)})\right). \quad (12)$$

Grass PFTs

The midday PAR that reaches the grass layer par_{grass} is calculated every day as follows, where $lai_{(p)}$ is the leaf area index of woody PFT p in this plot:

$$par_{grass} = (par_{direct} + par_{diffuse}) \times \exp\left(-1.0 \times \sum_{p=1}^{woody-pft} (EK_{(p)} \times lai_{(p)})\right). \quad (13)$$

This equation assumes that a tree with uniform foliage distributes PAR evenly over the grass

layer. As shown in the equation below, $eK_{(p)}$ is the light attenuation coefficient for the direction of the sun at midday. It is calculated every day as a function of solar angle at midday sl_{hgt} (see Appendix A2 for the calculation) and the light attenuation coefficient for vertical direction $EK_{(p)}$:

$$eK_{(p)} = EK_{(p)} / \{0.86 \sin(sl_{hgt})\}. \quad (14)$$

The horizontal line of $0.86 \times sl_{hgt}$ equally divides daily sum of solar radiation into two, when daily changes of solar angle and solar radiation are \sin and \sin^2 , respectively. We should point out that equation 13 should underestimate the par_{grass} , because tree leaves are unevenly distributed in the virtual forest and radiation is exponentially attenuated by the leaves. We chose the present approximation, however, to avoid time-consuming calculation of PAR distribution at the grass layer.

Photosynthesis

To compute photosynthesis values, the SEIB-DGVM assumes that environmental conditions other than PAR intensity (e.g. air temperature, CO₂, and water) are equal among all the leaves, all day. The single-leaf photosynthetic rate is formulated as a simple Michaelis-type function of the intensity of PAR, par :

$$p_{single} = \frac{p_{sat} \times lue \times par}{p_{sat} + lue \times par}. \quad (15)$$

, where $psat$ and lue are the light-saturated photosynthetic rate and light-use efficiency,

1 respectively (see Appendix A4 for the calculation).

2 **Woody PFTs**

3 According to Kuroiwa (1979), a daily change in PAR can be approximated by a sine square
 4 function as follows, where $dlen$ is day length (hour), and x and par_l are intensity of PAR on
 5 crown disk l at time t (hour from sunrise) and at midday, respectively:

$$6 \quad x = par_l \times \sin^2\left(\pi \times \frac{t}{dlen}\right). \quad (16)$$

7 By combining equations 16 and 15, and integrating the resultant equation into day length, the
 8 daily photosynthetic production on crown disk l , $gpp_{(l)}$, is obtained as follows, where constant
 9 $12 \cdot 10^{-6} \cdot 3600 / 0.41505$ is the unit converter from [$\mu\text{mol CO}_2 \text{ m}^{-2} \text{ s}^{-1}$] to [$\text{g DM m}^{-2} \text{ hour m}^{-2}$
 10 s^{-1}] and la_l is the leaf area within crown disk l :

$$11 \quad \begin{aligned} gpp_{(l)} &= 12 \times 10^{-6} \times 3600 \times \frac{1}{0.41505} \times la_{(l)} \times \int_0^{dlen} p_{single} dt \\ &= 0.090936 \times la_{(l)} \times dlen \times p_{sat} \times \left(1 - \frac{1}{\sqrt{1 + lue \times par_{(l)} / p_{sat}}}\right). \end{aligned} \quad (17)$$

12 Using 17, the daily photosynthetic production is obtained for each crown disk of each
 13 individual. These values are summed for each individual tree, and then added to the available
 14 resource of the tree, $mass_{available}$.

15 **Grass PFTs**

Grass leaves are assumed to be uniformly distributed within the grass layer. Thus, PAR of time t (hour from sunrise) at cumulative grass LAI y ($\text{m}^2 \text{m}^{-2}$) is calculated as follows, where par_{grass} is PAR at the surface of the grass layer at midday:

$$x = par_{grass} \times \sin^2\left(\pi \frac{t}{dlen}\right) \times e^{-eK \times y} . \quad (18)$$

By combining equations 18 and 15, and integrating the resultant equation into t and y , the daily gross primary production of the grass layer, gpp_g , is calculated as follows (Kuroiwa, 1979), where lai_g is the leaf area index of the grass layer ($\text{m}^2 \text{m}^{-2}$):

$$\begin{aligned} gpp_g &= 0.090936 \times \int_{y=0}^{lai_g} \int_{t=0}^{dlen} p_{single} dt dy \\ &= 0.090936 \times \frac{2 \times dlen \times p_{sat}}{eK} \times \ln \left(\frac{1 + \sqrt{1 + \frac{par_{grass} \times eK \times lue}{p_{sat}}}}{1 + \sqrt{1 + \frac{par_{grass} \times eK \times lue}{p_{sat}} e^{-eK \times lai_g}}} \right) . \end{aligned} \quad (19)$$

The daily photosynthetic production is added to available resource of grass PFTs, $gmass_{available}$.

Canopy Conductance

To compute single-leaf stomatal conductance gs , the SEIB–DGVM adopts a semi empirical model by Ball et al. (1987), modified by Leuning (1995), where $co2_{atm}$ is atmospheric CO_2 concentration, $co2_{cmp}$ is the CO_2 compensation point, and vpd is the vapor pressure deficit between saturated and actual vapor pressures:

$$gs = GS_{b1} + \frac{GS_{b2} \times p_{single}}{(co2_{atm} - co2_{cmp})(1 + vpd / GS_{b3})}. \quad (20)$$

Here, GS_{b1} , GS_{b2} , and GS_{b3} are PFT-specific parameters. In the model, vpd , $co2_{atm}$, and $co2_{cmp}$ are updated every day, according to Appendix A1 and A4. For each crown disk l of each tree n , mean daytime stomatal conductance ($gs_{mean(l,n)}$ in $\text{mol H}_2\text{O m}^{-2} \text{ s}^{-1}$) is obtained by combining equations 15, 16, and 20, and integrating the resultant equation into time t , averaged over the daytime:

$$gs_{mean(l,n)} = GS_{b1} + \frac{GS_{b2} \times p_{sat}}{(co2_{atm} - co2_{cmp})(1 + vpd / GS_{b3})} \left(1 - \frac{1}{\sqrt{1 + lue \times par_{(l,n)} / p_{sat}}} \right) \quad (21)$$

Thus, mean daytime and whole forest stomatal conductance of woody PFTs, $ccon_{wood}$ (in $\text{mol H}_2\text{O m}^{-2} \text{ s}^{-1}$), is calculated as follows, where $AREA$ is the area of the simulation plot (m^2):

$$ccon_{wood} = \sum_n \sum_l (gs_{mean(l,n)} \times la_{(l,n)}) / AREA. \quad (22)$$

The mean daytime stomatal conductance for grass PFTs, $ccon_{grass}$ (in $\text{mol H}_2\text{O m}^{-2} \text{ s}^{-1}$), is obtained by combining equations 15, 18, and 20, and integrating the resultant equation into daytime and cumulative LAI.

$$ccon_{grass} = GS_{b1} \times lai_g + \frac{GS_{b2} \times p_{sat}}{(co2_{atm} - co2_{cmp})(1 + vpd / GS_{b3})} \times \frac{2}{eK} \times \ln \left(\frac{1 + \sqrt{1 + \frac{par_{grass} \times eK \times lue}{p_{sat}}}}{1 + \sqrt{1 + \frac{par_{grass} \times eK \times lue}{p_{sat}} e^{-eK \times lai_g}}} \right) \quad (23)$$

We defined the sum of $ccon_{wood}$ and $ccon_{grass}$ as the mean daytime stomatal conductance of this plot ($ccon$ in $\text{mol H}_2\text{O m}^{-2} \text{ s}^{-1}$).

Growth Respiration

For plants to grow, they require carbohydrates both for their plant-body construction and for biosynthesis. Here, we define construction cost as the required biomass per actual growth (g DM g DM^{-1}). Thus, the amount of growth respiration of organ o is $(RGo - 1.0) \cdot \Delta mass_o$, where RGo is the construction cost of organ o and $\Delta mass_o$ is an biomass increment of organ o . Construction cost can be estimated by combining data on the biochemical composition of organs with knowledge on the biochemical costs of synthesis of all the major compounds, including cellulose, hemicellulose, lignin, protein, lipids, and organic acids (Lambers et al., 1998). Applying this method, Poorter (1994) collected biochemical composition data on various plant species, and then estimated the construction cost of leaves (1.56, mean value of 123 species), stems (1.44, mean value of 38 species), and roots (1.34, mean value of 35 species). Our model employs these parameters with the following two modifications: for grass PFTs, leaves and stems are grouped together as an 'leaf' and thus the two values are averaged (i.e., their collective construction cost is 1.50); the above parameters of Poorter (1994) are estimated mainly from grass species, so we employ 1.68 as the construction cost of a woody stem, because lignin synthesis requires a high expenditure of energy. This value is taken from

Penning de Vries (1975), but modified by changing the nitrogen source to NO_3 as in Poorter (1994).

Forming and utilizing storage resources ($mass_{stock}$ for woody PFTs and $gmass_{stock}$ for grass PFTs) incur metabolic costs such as the synthesis of a storage organ and remobilization of the nutrients within it (Lambers et al., 1998). We could not find any representative estimates that could be applied to a wide variety of plant species; thus, we assumed that 10% of the biomass is consumed while forming storage structures, and another 10% of the biomass of the storage structure is consumed while utilizing those resources ($RG_{stockin} = 1.1$; $RG_{stockout} = 1.1$).

Maintenance Respiration

In our simulations, maintenance respiration occurs every day irrespective of phenology phase. The carbohydrates required for maintenance respiration is first charged to the available resource and then the remaining requirements are charged to the stock resource. When the sum of these two resources of carbohydrate is not enough to cover the amount charged, 1% of the biomass of all of the living organs is removed. The removed biomass of sapwood changes to heartwood, while the removed biomass of other organs enters the litter pool. Note that maintenance respiration does not occur in heartwood or the stock resource.

For a wide variety of plant organs, the maintenance respiration rate is linearly related to the nitrogen content of living tissue (Ryan, 1991). Incorporating this tendency into our model, we calculate the daily maintenance respiration of an organ o as follows, where constant RM is the specific respiration rate at 15.0°C ($\text{g DM g N}^{-1} \text{ day}^{-1}$) and assumed to be 0.10 for all PFT, PN_o is the nitrogen content per biomass of organ o , tmp is air temperature for aboveground organs

and soil temperature for underground organs, and qt represents the temperature sensibility:

$$RM \times (mass_o \times PN_o) \times \exp\left[\frac{\ln(qt)}{10}(tmp - 15.0)\right]. \quad (24)$$

The temperature sensibility was formulated according to Yokota and Hagihara (1996), as follows:

$$qt = 2.0 \times \exp(-0.009(tmp - 15.0)). \quad (25)$$

First, we estimated the nitrogen content of the leaves PN_f for each PFT (Appendix B6) based on a data set from Wright et al. (2004). However, because this data set does not contain a value for boreal needle-leaved deciduous trees (BoND), the value of PN_f for this PFT is taken from an empirical regression equation by Reich et al. (1997), assuming a leaf longevity of three months. Then, assuming that the relative proportions of nitrogen in each organ for any particular PFT are linearly correlated, we calculated PN_s and PN_r as follows, where the coefficients 0.145 and 0.860 are employed by Friend et al. (1997):

$$PN_s = 0.145 \times PN_f \quad (26)$$

$$PN_r = 0.860 \times PN_f \quad (27)$$

Turnover

To account for the turnover of organic matter, constant fractions of leaves and fine roots are transformed into litter, while those of sapwood are transformed to heartwood. This turnover

occurs every simulation day irrespective of phenology phase. Appendix B6 shows the PFT-specific turnover rates of leaves TO_f ; the data set, which is taken from Wright et al. (2004), does not contain a value for boreal needle-leaved deciduous trees (BoND), so the leaf turnover rate of BoND is assumed to be 4 year^{-1} (i.e., a leaf longevity of three months). For deciduous PFTs, leaf turnover rates are corrected as follows, because they drop all leaves at the end of growth phase: $\max[0.0, TO_f - 365 / (\text{growth days in the last year})]$. We also employed this corrected turnover rate for calculation of daily maintenance cost of leaves in the equation 35. The turnover rate of sapwood TO_s is assumed to be 0.05 year^{-1} for all PFTs, except for BoNS, of which sapwood diameter is assumed to be $\min[dbh, 0.0188]$ (in m). The turnover rate of fine roots TO_r is taken from Gill and Jackson (2000).

Phenology

Every deciduous PFT in the model has two phenology phases: a growth phase and a dormant phase. Foliation and growth of deciduous PFTs only occurs during the growth phase. The criteria for switching between the two phases, and the procedure of phase change, are described below.

From Dormant Phase to Growth Phase

Each PFT is classified into the following phenology types, which differ in sub models. A daily computational time step is applied to each sub model.

- Summer green broad-leaved woods (TeBS, BoBS)

One of the phenology control variables is $gdd5_{Jan}$, which sums the daily mean air temperature

above 5°C starting on 1 January (for the northern hemisphere) and 1 July (for the southern hemisphere). Trees change from the dormant phase to the growth phase when $gdd5_{Jan}$ exceeds $-68 + 638 \times \exp(-0.01 \times i)$, where i is the sum of the days for which the mean air temperature is below 5°C, starting on 1 November (for the northern hemisphere) and 1 May (for the southern hemisphere). Thus, the number of cold days affects the number of days required for phenology change. This sub model is taken from Botta et al. (2000), which is based on the distribution of leaf onset date estimated from remote sensing data. We also assumed that the day of the year (doy) of the switch is within the range of 'latitude + 30' to 'latitude + 130' for the northern hemisphere, and '212 – latitude' to '312 – latitude' for the southern hemisphere.

- Summer green needle-leaved woods (BoNS)

Foliation phase starts when sum of air temperature above 4.1 degree Celsius from January 1 exceeds 65. This sub model is taken from Picard et al. (2005), which is based on the distribution of leaf onset date estimated from remote sensing data.

- Raingreen woody PFT (TrBR)

When 10 day running average of $stat_{water}$ exceeds 0.5, the dormant phase changes into growth phase.

- Grass PFTs (TeH, TrH)

When optimum leaf area index (lai_{opt} ; formulas described in the section titled 'Growth Procedure of Woody PFTs') exceeds 0 for preceding 7 days, the dormant phase changes into the growth phase.

For the first 14 days (10 days for BoNS) of the growth phase, all of the stock resource is consumed, transformed into available resource at a constant rate. For grass PFTs, this transformation is paused when the optimal leaf area index, lai_{opt} , is reached.

4 From Growth Phase to Dormant Phase

At day 60 after the leaf onset date, leaf phenology can change to the dormant phase. When this occurs, all of the leaves of woody PFTs except for BoNS and grass PFTs are instantly shed as litter. At this moment, if the stock resource does not satisfy the minimum value (100 g individual⁻¹ for woody PFTs, 50 g m⁻² for grass PFTs), the deficit is supplemented from the litter pool. Each deciduous PFT have distinct condition to change from the growth phase to the dormant phase. When a deciduous PFT does not satisfy the condition, it acts as *de facto* evergreen PFT.

• Temperate summer green broad-leaved woods (TeBS)

The phenology phase is declared dormant if the 10-day running mean of air temperature falls below 9°C or below the 10-year running mean of the coldest month temperature + 5°C.

• Boreal summer green broad-leaved woods (BoBS)

The phenology phase is declared dormant if soil temperature falls below 2°C. This criteria is from Arora and Boer (2005),

• Boreal summer green needle-leaved woods (BoNS)

When daily mean air temperature becomes less than 4 °C for successive 7 days, leaf defoliation phase occurs, which lasts 14 days. While the defoliation phase, all leaves are

1 transformed into litter at a constant rate.

2 • Raingreen woody PFT (TrBR)

3 The phenology phase is declared dormant when 10 day running average of $stat_{water}$ falls below
4 10.

5 • Grass PFTs (TeH, TrH)

6 The phenology phase is declared dormant if optimum leaf area index (lai_{opt}) falls below 0 for
7 preceding 7 days.

8 Growth procedure of woody PFTs

9 The growth process of woody PFTs consists of three procedures with daily, monthly, and
10 annual time steps. Each procedure employs a dynamic allocation scheme to reduce the
11 parameter requirements.

12 Daily Computation

13 During the growth phase, while resource availability ($mass_{available}$) is greater than 0, the
14 following procedures are executed for each individual tree every simulation day.

15 (1) If the fine root biomass ($mass_{root}$) is less than is required by the functional balance
16 ($mass_{leaf}/FRratio$), the deficit is supplemented from $mass_{available}$. Here, $FRratio$ is the ratio of
17 leaf biomass to fine root biomass satisfying the functional balance. $FRratio$ is assumed to be
18 1.50 for all woody PFTs and 1.00 for all grass PFTs.

(2) The stock resource ($mass_{stock}$) is supplemented until it becomes equal to the existing leaf mass ($mass_{leaf}$). However, this step is skipped for the first 30 days of the growing season.

(3) The final step of the daily growth procedure is foliation. There are three constraints on the maximum leaf biomass for each individual: crown surface area (max_1), cross-sectional area of sapwood (max_2), and available resource (max_3). These maximum values (in g DM) are defined as follows:

$$max_1 = (crown_{area} + \pi \times crown_{diameter} \times crown_{depth}) \times LAm_{max}/SLA \quad (28)$$

$$max_2 = ALM_l \times \left[\pi \left(\frac{dbh_{heartwood}}{2} + \frac{dbh_{sapwood}}{2} \right)^2 - \pi \left(\frac{dbh_{heartwood}}{2} \right)^2 \right] / SLA \quad (29)$$

$$max_3 = mass_{available}/RG_f, \quad (30)$$

where the constant SLA is the PFT-specific leaf area per unit biomass (Appendix B4). SLA is primary taken from data of Wright et al. (2004), but it does not include a value for boreal needle-leaved deciduous trees (BoND); thus, the SLA value for this type is derived from an empirical regression equation from Reich et al. (1997), assuming a leaf longevity of three months. LAm_{max} is the PFT-specific maximum leaf area per unit crown surface area excluding the bottom soffit. ALM_l is a constant that represents the required area of transport tissue per unit leaf area (Shinozaki et al. 1964a, b). If the current leaf area is less than the $\min(max_1, max_2, max_3)$, the deficit is supplemented from $mass_{available}$.

In case of BoNS, leaf mass is simply given as a function of diameter at breast height, 330 +

1 50580 dbh^2 (in g DM). Also, leaf onset only occurs for initial 30 days of foliation phase.

2 **Monthly Computation**

3 The monthly process of tree growth is outlined below, in the order of execution. For
4 deciduous PFTs, this procedure is omitted during the dormancy phase and for the first three
5 weeks of the growing phase.

6 (1) Reproduction: If total woody biomass is more than 10 kg, 10% of the available resource
7 ($mass_{available}$) is transformed into litter.

8 (2) Trunk growth: All of the remaining resource is used for sapwood biomass ($mass_{sapwood}$)
9 growth. There is no direct allocation to heartwood, which is produced indirectly by slowly
10 converting sapwood. In case of BoNS, resource for producing trunk is diminished by
11 multiplying following reduction factor $1.0 - (dbh/0.5)^2$. This equation assumes that stem
12 growth efficiency becomes lower when dbh approaches to its maximum limit at 0.5m. The
13 reduced resource is consumed by maintenance respiration.

14 Increments of sapwood biomass are accompanied by growth in sapwood diameter ($dbh_{sapwood}$)
15 and trunk height ($height$). These increments ($\Delta dbh_{sapwood}$ and $\Delta height$) must satisfy the
16 following two trunk mechanics.

17 (A) Trunk mechanics 1: a relationship between trunk biomass and trunk geometry.
18 Trunk biomass, a function of tree height ($height$) and trunk diameter, is calculated as follows,
19 where ALM_3 is dry mass per unit timber volume (in g DM m^{-3}):

$$mass_{trunk} = ALM_3 \times \pi \left(\frac{dbh}{2} \right)^2 \times height \quad (31)$$

The value of ALM_3 for BoNS was obtained from Schulze et al. (1995), while those of broad-leaved PFTs and evergreen needle-leaved PFTs were calculated by averaging 46 broad-leaved woody species and 24 needle-leaved woody species from Japan; the data were obtained from a table in *The Handbook of Wood Industries* (FFPRI, 1982). It should be noted that the table excluded pioneer woody species, which typically produce low-density timber, and that the SEIB–DGVM assumes that the trunk has a cylindrical shape that extends to the top of the crown (Fig. 1). Thus, the estimated trunk biomass should exceed the actual biomass for the same trunk diameter at bottom with tapered trunk shape; however, because the model includes branches and coarse roots as trunk biomass, this simplification might be justified.

In case of BoNS, $mass_{trunk}$ is given by

$$\min \left[1.5 \left(4670000 \pi \left(\frac{dbh}{2} \right)^2 - 11300 \right), 190(100dbh)^{1.7} + 42.8(100dbh)^{1.79} + 171(100dbh)^{1.67} \right] \quad (31')$$

(B) Trunk mechanics 2: a relationship between trunk diameter and maximum tree height for that diameter, calculated as follows, where the parameters HGT_s and HGT_{max} are the initial growth slope and the maximum tree height for an infinite trunk diameter, respectively:

$$height \leq \left[\frac{1}{HGT_s \times (dbh_{sapwood} + dbh_{heartwood})} + \frac{1}{HGT_{max}} \right]^{-1} \quad (32)$$

As shown in Appendix B4, $HGTs$ and HGT_{max} values for tropical trees and temperate broad-leaved trees are taken from Kohyama et al. (1999); those for temperate needle-leaved trees are from T. Nishimura (unpublished data, 2005); those for BoNS are from Schulze et al. (1995); and for other boreal trees are from Takahashi et al. (2001). In the model, the crowns of different trees cannot occupy the same space. Thus, when the crowns of neighboring trees interfere with tree height, only the trunk diameter expands.

(3) Expansion of a cross-sectional area of the crown:

We used relationships between stem diameter and crown cross-sectional area, based on the inversion of Reineke's rule (Zeide, 2001). Crown expansion is calculated as follows, where the constant ALM_2 is assumed to be 100.0 for every needle-leaved PFT and 200.0 for every broad-leaved PFT:

$$crown_{area} \leq ALM_2 \times (dbh_{sapwood} + dbh_{heartwood})^{1.6}. \quad (33)$$

In case of BoNS, we applied following equation.

$$crown_{area} \leq 80 \times (dbh_{sapwood} + dbh_{heartwood}). \quad (33')$$

The crown diameter has two constraints: it can neither exceed its maximum limit (CD_{max}) nor expand into neighboring crowns.

Annual Computation

On the last day of each year, the height of the lowest branch increases as a result of purging crown disks, or self pruning of branches, at the bottom of the crown layer. This procedure is conducted even if the tree is in the dormancy phase. A maximum of 10 crown disks can be pruned at one time, each at a depth of 10 cm. Consequently, and because elongation of the lowest branch is linked to crown pruning, the maximum increase in height of the lowest branch is 100 cm year⁻¹. To determine the number of crown disks to purge, we first calculate a variable, $stat_{leaf}$, which represents the expected profit of maintaining a crown disk (g DM day⁻¹), as follows, where gpp_l is the daily photosynthetic production of a crown disk and $cost$ is the daily maintenance cost per unit leaf biomass (in g DM g DM day⁻¹):

$$stat_{leaf} = gpp_l - cost \times \frac{la}{SLA} \times \frac{1}{10 \times crown_{depth}}. \quad (34)$$

The $cost$ variable is calculated daily for each PFT as follows, where $r1$ and $r2$ are the daily maintenance respiration rates of leaves and fine roots, respectively (g g⁻¹ day⁻¹), derived from equation 24 for each PFT:

$$cost = \left(r1 + RG_f \times \frac{TO_f}{365} \right) + \left(r2 + RG_r \times \frac{TO_r}{365} \right) \frac{1}{FRratio}. \quad (35)$$

Then, the annual mean of $stat_{leaf}$ for each of the 10 crown groups (1–10 successive disks from the crown bottom) for each tree is calculated. These values are divided by the annual mean of $stat_{leaf}$ of the top crown disk of each tree, and then this value is used to select disks for purging. Those with values less than ALM_4 are selected for pruning; of these, the group that includes the largest number of crown disks is pruned. It should be noted that pruning is also constrained by $crown_{depth}$, which must always exceed 10 (i.e., >100 cm) and that once a crown

1 disk is pruned, it cannot reestablish (i.e., the height of the lowest branch cannot decrease).

2 In case of BoNS, crown depth (m) is simply assumed to be $\min[10, height]$.

3 On the last day of each year, the crown center moves horizontally toward the most open
4 direction. This crown movement represents the fact that trees extend their branches into open
5 and bright spaces. Without introducing this plasticity, interference among crowns severely
6 limits the number of tall trees, because crowns of different trees cannot occupy the same
7 space in the SEIB–DGVM. The maximum speed of crown movement is assumed to be 20 cm
8 year^{-1} , and the maximum distance of the movement is equal to half of the crown radius (i.e.,
9 the distance between the bole and crown centers is less than half of the crown radius).

10 Growth Process of Grass PFTs (Daily Computation)

11 During the growth phase, while resource availability ($gmass_{available}$) is greater than 0, the
12 following procedures are executed every simulation day.

13 (1) If root biomass ($gmass_{root}$) is less than that required by the functional balance
14 ($gmass_{leaf}/FRratio$), the deficit is supplemented.

15 (2) The stock resource ($gmass_{stock}$) is supplemented until it becomes equal to the existing leaf
16 biomass ($gmass_{leaf}$). This step is omitted for the first 30 days of the growing season.

17 (3) The leaf biomass ($gmass_{leaf}$) is supplemented until the leaf area index of the PFT (lai_g)
18 reaches a weekly running mean equal to the optimal leaf area index lai_{opt} , which maximizes

daily net primary production, $gpp_g - cost \times lai_g / SLA$ (derived from equations 19 and 34). This variable is calculated as follows, where $cost$ is the cost of maintaining leaves per unit leaf mass per day (see equation 34 for the definition):

$$lai_{opt} = \frac{\ln par_{grass} - \ln \left\{ \frac{p_{sat}}{lue} \left[\left(1 - \frac{cost / SLA}{0.09093 \times dlen \times p_{sat}} \right)^{-2} - 1 \right] \right\}}{eK}. \quad (36)$$

(4) All remaining resource ($gmass_{available}$) is used for reproduction, and then transformed into litter. This step is omitted for the first 30 days of the growing season and when the stock resource is less than 100 g DM m⁻².

Mortality (Except Death by Fire)

Mortality is explicitly modeled only for woody PFTs. On the last day of each simulation year, the overall death rate is calculated for each individual tree as a sum of mortality components, which consist of background mortality, heat stress, and bioclimatic limit. These components are derived from the LPJ-DGVM (Sitch et al., 2003). In addition to the above parameters, a tree dies if the NPP of the previous year is less than 10 DM g or if the trunk diameter is more than 1.0 m. It is also assumed that newly established trees do not die in their first year.

Background mortality is related to growth efficiency, which seems to be a sensitive indicator of resistance to environmental stress (Warning, 1983). Although there is no standard formula for background mortality, the model assumes the following, where $anpp$ is the annual sum of net primary production (g DM), la_{mean} is the mean leaf area of the previous year (m²), and M_1 (≤ 1.0) and M_2 (≥ 1.0) are PFT-specific mortality coefficients:

$$\frac{M_1}{M_2^{\frac{anpp}{la_{mean}}}}. \quad (37)$$

Mortality by heat stress is determined only for boreal woody PFTs (BoNE, BoNS, BoBS). This mortality component, which is based on the sum of daily temperatures, is calculated as follows, where $tmp_{air(d)}$ is the air temperature on day d of the year:

$$\min\left[1.0, \sum_{d=1}^{365} \max(0.0, tmp_{air(d)} - 23.0) / 300\right]. \quad (38)$$

Mortality by bioclimatic limit restricts the climate range in which each PFT can survive. If the 20-year mean of the coldest month temperature is less than the PFT-specific limit TC_{min} , all individuals of the PFT die immediately. Boreal needle-leaved summergreen trees (BoNE) have an additional bioclimatic limit: if the 20-year mean of (warmest–coldest monthly air temperature) is less than 43°C, all trees of the PFT die. Biomass of dead trees is forming new litter.

Disturbance by Fire

Fire is the only disturbance currently incorporated in the SEIB–DGVM. We employed the global fire model of Thonicke et al. (2001), which was developed for the LPJ–DGVM. On the last day of each simulation year, if the fuel load (litter + aboveground biomass) satisfies the minimum threshold (200 g C m⁻²), the probability of fire is calculated as a function of the moisture content of soil layer 1 as follows:

$$s \times \exp\left(\frac{s-1}{0.45(s-1)^3 + 2.83(s-1)^2 + 2.96(s-1) + 1.04}\right), \quad (39)$$

, where variable s is

$$s = \sum_{day=1}^{365} \exp\left[-\pi\left(\frac{pool_{w(1)}}{W_{sat} \times Depth_{(1)}} \times \frac{1}{m_e}\right)^2\right] / 365. \quad (40)$$

Variable m_e in equation 40, which takes into consideration the difference in fire extinction efficiency between woody and grass PFTs, is defined as $0.3 \times (\text{aboveground biomass of trees} / \text{total aboveground biomass}) + 0.2 \times (\text{leaf biomass of grass} / \text{total aboveground biomass})$. The model also assumes that fire cannot occur in two consecutive years.

The fraction of individuals killed in a fire depends on PFT fire resistance (M_3 , Appendix B5). During a fire, all leaf biomass of grass, all leaf biomass of dead and surviving trees, half of the trunk biomass of dead trees, and half of the litter pool are released into the atmosphere as CO_2 , while the remaining biomass of dead trees is transformed into litter. In response to fire, the phenology phase of all deciduous PFTs changes to dormant (they reenter the growth phase as described previously in the section titled ‘Phenology’). If the stock resource of grass PFTs ($gmass_{stock}$) does not satisfy the minimum value (50 g DM m^{-2}) after fire, the deficit is supplemented from litter.

Soil Respiration

The decomposition of litter and soil organic carbon is calculated for each month. The SEIB–DGVM employs the soil respiration module of the DEMETER-1 (Foley, 1995) with

some simplifications. The average annual decomposition rate of litter pool k_l is calculated as follows, where aet is the actual evapotranspiration in the previous year:

$$k_l = \min\left(1.0, \frac{10^{(-1.4553+0.0014175 \times aet)}}{12}\right). \quad (41)$$

Seventy percent of the decomposed litter carbon is released into the atmosphere as CO_2 , and the remaining 30% becomes soil organic carbon. The partitioning coefficients for soil organic carbon flowing into the fast and slow decomposition pools are 0.985 and 0.015, respectively.

According to Foley (1995), the mean turnover rates for the fast and slow soil organic carbon (TO_{fast} , TO_{slow}) at 20°C and ample soil moisture are $1/15 \text{ year}^{-1}$ and $1/750 \text{ year}^{-1}$, respectively. Actual monthly turnover rates ($k_n \text{ month}^{-1}$), which are adjusted according to soil environment, are calculated as follows, where g and f are functions of the monthly mean air temperature and soil moisture, respectively:

$$k_n = \left[\frac{TO_n}{12} \times g(tmp_{soil}) \times f(pool_{w(l)}) \right] \quad (42)$$

These functions are defined as follows:

$$g(tmp_{soil}) = \exp\left(308.56 \times \left(\frac{1}{66.02} - \frac{1}{tmp_{soil} + 46.02}\right)\right) \quad (43)$$

$$f(pool_{w(l)}) = 0.25 + 0.75 \left(\frac{pool_{w(l)}}{W_{sat} \times Depth_{(l)}} \right) \quad (44)$$

1 In Foley (1995), the temperature effect $g(tmp_{soil})$ is an exponential function. However, this
2 underestimates the soil turnover rate for cold regions, and thus we employ the function of
3 Lloyd and Taylor (1994). All decomposed soil organic carbon is released into the atmosphere
4 as CO₂.

1 Appendix A

2 A1. Atmospheric environments (computed daily)

3 Atmospheric conditions were calculated daily based on input climate data. Air pressure (ap in
4 hPa) was approximated by site altitude (ALT in m) and air temperature (tmp_{air} in °C):

$$5 \quad ap = 1013.25 \times \exp\left(\frac{-0.2838472 \times ALT}{8.3144(tmp_{air} + 273.15)}\right), \quad (A1)$$

6 where the multiplier 1013.25 is the control air pressure (in hPa) at sea level at 15°C, and the
7 multiplier 8.3144 is the universal gas constant (in J mol⁻¹ K⁻¹). Actual vapor pressure (vp in
8 hPa) was a function of air pressure ap and humidity $humid$ (g g⁻¹):

$$9 \quad vp = \frac{ap \times humid}{0.622 + 0.378 \times humid}, \quad (A2)$$

10 The saturated vapor pressure vp_{sat} (hPa) was given by Tetens' equation:

$$11 \quad vp_{sat} = 6.1078 \times 10^{\frac{7.5tmp_{air}}{237.3+tmp_{air}}} \quad (tmp_{air} > 0.0) \quad (A3)$$

$$12 \quad vp_{sat} = 6.1078 \times 10^{\frac{9.5tmp_{air}}{265.3+tmp_{air}}} \quad (tmp_{air} \leq 0.0). \quad (A4)$$

13 The vapor pressure deficit vpd (hPa) is the difference between saturated and actual vapor

1 pressures:

$$2 \quad vpd = vp_{sat} - vp. \quad (A5)$$

3 The slope of saturated vapor pressure $slope_{vps}$ (hPa °C⁻¹) is:

$$4 \quad slope_{vps} = \frac{6.1078 \times (2500 - 2.4tmp_{air})}{0.4615(tmp_{air} + 273.15)^2} \times 10^{\frac{7.5tmp_{air}}{237.3 + tmp_{air}}} \quad (tmp_{air} > 0.0) \quad (A6)$$

$$5 \quad slope_{vps} = \frac{6.1078 \times 2834.0}{0.4615(tmp_{air} + 273.15)^2} \times 10^{\frac{9.5tmp_{air}}{265.3 + tmp_{air}}} \quad (tmp_{air} \leq 0.0). \quad (A7)$$

6 The density of air $dnsa$ (kg m⁻³) is:

$$7 \quad dnsa = 1.293 \frac{ZAT}{tmp_{air} + ZAT} \times \frac{ap}{1013.25} \times \left(1 - 0.378 \frac{vp}{ap} \right). \quad (A8)$$

8 A2. Solar radiation (computed daily)

9 Angular solar elevation above the horizontal at midday (sl_{hgt}) was calculated by the following

10 equations:

$$11 \quad \sin(sl_{hgt}) = \sin(LAT) \times \sin(sl_{dec}) + \cos(LAT) \times \cos(sl_{dec}), \quad (A9)$$

where LAT is the site latitude ($-90 \leq LAT \leq 90$ in degree) and sl_{dec} is the solar declination of the earth's orbit in degrees. sl_{dec} has a maximum value of 23.4 on the summer solstice, and a minimum value of -23.4 on the winter solstice, and a value of 0 on equinox days; thus, it can be approximated by the following equation:

$$sl_{dec} = 23.4 \sin(360 \times (doy - 81) / 365), \quad (A10)$$

where doy is the days of the year (1–365, ignoring leap years). Using sl_{dec} , the hourly angle of the sun from sunrise to midday can be calculated as $\arccos(-\tan(LAT) \times \tan(sl_{dec}))$; thus, the day length in hours ($dlen$) will be:

$$dlen = 2 [\arccos(-\tan(LAT) \times \tan(sl_{dec})) / 15]. \quad (A11)$$

Shortwave radiation at the top of the atmosphere at midday (rad_{intact} in $W m^{-2}$) is a function of sl_{hgt} :

$$rad_{intact} = 1367 \times \sin(sl_{hgt}) \times (ESD_{mean}/ESD)^2, \quad (A12)$$

where the multiplier 1367 is a solar constant (in $W m^{-2}$), ESD is the distance between the sun and the earth (in km), and ESD_{mean} represents the annual mean ESD ($=1.46 \cdot 10^8$ km). $(ESD_{mean}/ESD)^2$ can be approximated by:

$$(ESD_{mean}/ESD)^2 = 1.000111 + 0.034221 \cos(x) + 0.00128 \sin(x) + 0.000719 \cos(2x) + 0.000077 \sin(2x), \quad (A13)$$

where x is the seasonal angle of the earth's orbit ($x = 360 \times doy/365$). In the troposphere, the incident solar radiation rad_{intact} ($W m^{-2}$) is attenuated by clouds and airborne particles. This effect has been empirically formulated as a function of cloud cover ($0.0 \leq cloud \leq 0.8$) by Itoh (personal communication) based on NCEP/NCAR data, as follows:

$$rad = rad_{intact} \times (0.8964 - 0.5392 cloud), \quad (A14)$$

where rad is the amount of solar radiation that reaches to the biosphere (in $W m^{-2}$).

In addition to this attenuation effect on irradiance, scattering in the atmosphere optically alters the ratio between direct and diffuse radiation:

$$rad_{diffuse} = rad \times [0.958 - 0.982 (rad/rad_{intact})] \quad (A15)$$

$$rad_{direct} = rad - rad_{diffuse}, \quad (A16)$$

where $rad_{diffuse}$ and rad_{direct} are diffuse radiation and direct radiation within rad , respectively. Diffuse and direct radiation differ in their fractional content of photosynthetically active radiation (PAR: 400–700 nm) in the total spectrum; diffuse radiation contains 57%, while

direct radiation contains 43%. Thus, photosynthetic photon flux density of PAR is given by the following:

$$par_{diffuse} = 4.2 \times 0.57 \times rad_{diffuse} \quad (A17)$$

$$par_{direct} = 4.6 \times 0.43 \times rad_{direct} \quad (A18)$$

$$par = par_{diffuse} + par_{direct} \quad (A19)$$

where par is photosynthetically active radiation at midday (in $\mu\text{mol photon m}^{-2} \text{ s}^{-1}$), and $par_{diffuse}$ and par_{direct} are the diffused and direct radiation components of par . The multipliers 4.2 and 4.6 are for unit conversion from $[\text{W m}^{-2}]$ to $[\mu\text{mol photons m}^{-2} \text{ s}^{-1}]$ for diffuse and direct radiation, respectively (Larcher, 1995).

A3. Net Radiation (Computed Daily)

To estimate the transpiration rate of leaves and the evaporation rate of soil, the net radiation at vegetation ($radnet_{veg}$ in W m^{-2}) and at the soil surface ($radnet_{soil}$ in W m^{-2}) were calculated as:

$$radnet_{veg} = [rad \times (1 - albedo_{veg}) + radnet_{long}] \times (1 - ir) \quad (A20)$$

$$radnet_{soil} = [rad \times (1 - albedo_{soil}) + radnet_{long}] \times ir, \quad (A21)$$

1 where ir is the shortwave interception by leaves:

$$2 \quad ir = \exp\left(\sum_p^{pft} (-eK_p \times lai_p)\right) \quad (A22)$$

3 and $albedo_{veg}$ and $albedo_{soil}$ are the albedo of vegetation and the soil surface, respectively;
4 $albedo_{veg}$ was assumed to be 0.24 for forest biome and 0.15 for other biome (Jones 1992). On
5 the other hand, $albedo_{soil}$ was assumed be a function of soil albedo ($ALBEDO$) and the amount
6 of snow on the ground:

$$7 \quad albedo_{soil} = ALBEDO + (0.7 - ALBEDO)/[1 + \exp(-0.05(pool_{snow} - 70.0))]. \quad (A23)$$

8 The $radnet_{long}$ is net long-wave radiation, which is estimated by the following empirical
9 formula:

$$10 \quad radnet_{long} = 5.67 \times 10^{-8} \times (tmp_{air} + 273.15)^4 \times (1 - 0.65 \text{ cloud}) \times [0.39 + 0.058/(vp + \\ 11 \quad 1.0)], \quad (A24)$$

12 where the constant 5.67×10^{-8} is Stefan–Boltzmann's constant (in $W \text{ m}^{-2} \text{ K}^{-4}$).

13 A4. Parameters of Photosynthesis and Stomatal Conductance (Computed Daily)

14 Appendix B7 shows the definition of PFT-specific photosynthesis parameters. To estimate

photosynthesis and stomatal conductance, daily averages of photosynthetic rates (p_{ave} in $\mu\text{mol CO}_2 \text{ m}^{-2} \text{ s}^{-1}$) was calculated for grass layer and for each tree, using equation (15):

$$p_{top} = \frac{p_{sat} \times lue \times x}{p_{sat} + lue \times x}, \quad (\text{A25})$$

where p_{sat} is single-leaf photosynthetic rate under light saturation (in $\mu\text{mol CO}_2 \text{ m}^{-2} \text{ s}^{-1}$). x is the daily average of PAR receiving for grass layer (for grass PFTs) or for foliage of each tree (for woody PFTs) (in $\mu\text{mol photon m}^{-2} \text{ s}^{-1}$). lue is the light-use efficiency of photosynthesis (in $\text{mol CO}_2 \text{ mol photon}^{-1}$), which is formulated to conform to the data in Osmond et al. (1980) as follows:

$$lue = LUE \times \frac{52 - tmp_{air}}{3.5 + 0.75(52 - tmp_{air})} \times \frac{co2_{cell}}{90 + 0.6 \times co2_{cell}} \quad (\text{for } C_3 \text{ PFTs}) \quad (\text{A26})$$

$$lue = LUE \quad (\text{for } C_4 \text{ PFTs}), \quad (\text{A27})$$

where LUE is the potential maximum value, and $co2_{cell}$ is the intercellular CO_2 concentration (in $\mu\text{mol mol}^{-1}$). The single-leaf photosynthetic rate, p_{sat} , under light saturation (in $\mu\text{mol CO}_2 \text{ m}^{-2} \text{ s}^{-1}$), is calculated by multiplying its potential maximum of photosynthetic rate ($PMAX$) by the coefficients of temperature, CO_2 level, and soil water effects (ce_{tmp} , ce_{co2} , and ce_{water} , respectively):

$$p_{sat} = PMAX \times ce_{tmp} \times ce_{co2} \times ce_{water}. \quad (\text{A28})$$

ce_{tmp} , the temperature-dependent function of p_{sat} , is a bell-shaped curve that reaches the maximum (1.0) at the optimum temperature and tapers off in warmer or cooler temperatures (Raich et al., 1991):

$$ce_{tmp} = \frac{(tmp_{air} - T_{max})(tmp_{air} - T_{min})}{(tmp_{air} - T_{max})(tmp_{air} - T_{min}) - (tmp_{air} - t_{opt})^2}, \quad (A29)$$

where T_{max} , T_{min} , and t_{opt} are the PFT-specific maximum, minimum, and optimum temperature for photosynthesis, respectively (in °C). t_{opt} increases with the intercellular CO₂ concentration because of photorespiration:

$$t_{opt} = T_{opt0} + 0.01 \text{ } co2_{cell} \quad (A30)$$

where T_{opt0} is the minimum value of t_{opt} at a very low $co2_{cell}$. For grass PFTs, t_{opt} is assumed to be a 20-year running mean of air temperature in the growth phase (maximum range 10°C–30°C for TeH and 20°C–40°C for TrH), because grass PFTs includes a varieties of species adapted to a wide range of climatic zones.

The ce_{co2} , the CO₂-dependent function of p_{sat} , is expressed by a Michaelis-type function:

$$ce_{co2} = 0.30 + 0.70 \times \frac{co2_{cell} - co2_{cmp}}{KM + co2_{cell}} \quad (\text{for } C_3 \text{ PFTs}) \quad (A31)$$

$$ce_{co2} = 0.50 + 0.50 \times \frac{co2_{cell} - co2_{cmp}}{KM + co2_{cell}} \quad (\text{for } C_4 \text{ PFTs}), \quad (A32)$$

where KM is the coefficient of CO_2 concentration sensitivity; $co2_{cmp}$ is the CO_2 compensation point, which is adjusted by temperature for C_3 species (Brooks and Farquhar, 1985).

$$co2_{cmp} = CO2cmp \left[1 + 0.0451(tmp_{air} - 20) + 0.000347(tmp_{air} - 20)^2 \right] \quad (\text{for } C_3 \text{ PFTs}) \quad (A33)$$

$$co2_{cmp} = CO2cmp \quad (\text{for } C_4 \text{ PFTs}), \quad (A35)$$

where $CO2cmp$ is the control value of $co2_{cmp}$ at $20^\circ C$; ce_{water} , the water availability effect coefficient of p_{sat} , is calculated as follows:

$$ce_{water} = \sqrt{stat_{water}}. \quad (A35)$$

The midday leaf stomatal conductance of H_2O at the top of the leaf layer gs_{top} ($\text{mol } H_2O \text{ m}^{-2} \text{ s}^{-1}$), is obtained by equation 20:

$$gs_{top} = GS_{b1} + \frac{GS_{b2} \times p_{top}}{(co2_{atm} - co2_{cmp})(1 + vpd / GS_{b3})}, \quad (A36)$$

where GS_{b1} , GS_{b2} , and GS_{b3} are PFT-specific parameters; gs_{top} affects the intercellular CO_2 concentration ($co2_{cell}$ in $\mu\text{mol mol}^{-1}$) following Leuning (1990):

$$co2_{cell} = co2_{atm} - \frac{P_{top}}{gs_{top}/1.56}, \quad (A37)$$

where 1.56 is a factor to convert gs into CO_2 conductance. Using equations A25 through A37, we calculated p_{top} , lue , and gs_{top} of each PFT every simulation day.

A5. Soil water percolation (daily computation)

Water infiltration, percolation and runoff were simulated daily with a modified version of a submodel of MAPPS (Neilson, 1995), which is based on Darcy's law (Hillel, 1982). Calculations were made in the following order: (1) infiltration, (2) percolation from soil layer 1 to 2, (3) percolation from soil layer 2 to 3. We assumed that infiltration and percolation from soil layer 1 to 2 can only occur when soil temperature at 10cm depth is more than 0 °C. As well, soil water percolation from soil layer 2 to 3 can only occur when annual mean of soil temperature at 10cm depth is more than 0 °C.

Daily infiltrated water to soil layer 1, $pn_{(0)}$, is:

$$pn_{(0)} = prec_{rain} - ic + tw, \quad \frac{pool_{w(1)}}{Depth_{(1)}} \leq W_{mat} \quad (A38)$$

$$pn_{(0)} = (prec_{rain} - ic + tw) \left\{ 1 - \left[\frac{(pool_{w(1)}/Depth_{(1)}) - W_{mat}}{W_{sat} - W_{mat}} \right]^{1.4} \right\}, \quad W_{mat} < \frac{pool_{w(1)}}{Depth_{(1)}} \leq W_{fi} \quad (A39)$$

$$pn_{(0)} = 0.0, \quad W_{fi} < \frac{pool_{w(1)}}{Depth_{(1)}}, \quad (A40)$$

where W_{mat} , W_{sat} and W_{fi} are the soil moisture at matrix potential, saturation point, and field capacity, respectively. These are location-specific parameters. $Depth_{(n)}$ is the depth of soil layer n , which is assumed to be constant irrespective of location ($Depth_{(1)} = 500$ mm, $Depth_{(2)} = 1000$ mm, and $Depth_{(3)} = 1500$ mm). The constant 1.4 is an infiltration parameter, which is adjusted daily (unpublished data of Conklin and Neilson, 2005). All daily excess water at the soil surface is removed as runoff water.

Water in soil layer n is percolated to the next layer according to the following:

$$pn_{(n)} = K_{s1(n)} \left(pool_{w(n)} - W_{fi} \times Depth_{(n)} \right) \left(\frac{pool_{w(n)} / Depth_{(n)} - W_{fi}}{W_{sat} - W_{fi}} \right)^{K_{s2(n)}}, \quad W_{fi} < \frac{pool_{w(n)}}{Depth_{(n)}} \quad (A41)$$

$$pn_{(n)} = K_{u1(n)} \left(pool_{w(n)} - W_{mat} \times Depth_{(n)} \right) \left(\frac{pool_{w(n)} / Depth_{(n)} - W_{mat}}{W_{sat} - W_{mat}} \right)^{K_{u2(n)}}, \quad W_{mat} < \frac{pool_{w(n)}}{Depth_{(n)}} \leq W_{fi} \quad (A42)$$

$$pn_{(n)} = 0.0, \quad \frac{pool_{w(n)}}{Depth_{(n)}} \leq W_{mat} \quad (A43)$$

The coefficients $K_{u1(n)}$, $K_{u2(n)}$, $K_{s1(n)}$, and $K_{s2(n)}$ are adjusted daily (Appendix B8; unpublished

data of Conklin and Neilson, 2005). The actual amount of water allowed to percolate is the lesser of the calculated flux from a given layer (layer 1 or 2) or the available water-holding capacity ($W_{fi} \times Depth_{(n)} - pool_{w(n)}$) in the layer below (layer 2 or 3).

A6. Evapotranspiration (Computed daily)

The potential evaporation (ev_{pm}) and transpiration (tr_{pm}) are estimated by the Penman–Monteith method (Monteith and Unsworth, 1990), assuming an abundant water supply:

$$ev_{pm} = \frac{dlen \times 0.5 \times slope_{vps} \times radnet_{soil} + 24 \times 1012 \times dnsa \times vpd \times c_{aero}}{695 \{ slope_{vps} + 0.667(1.0 + c_{aero} / c_{soil}) \}}, \quad (A44)$$

$$tr_{pm} = \frac{dlen \times 0.5 \times slope_{vps} \times radnet_{veg} + dlen \times 1012 \times dnsa \times vpd \times c_{aero}}{695 \{ slope_{vps} + 0.667(1.0 + c_{aero} / c_{leaf}) \}} - ic, \quad (A45)$$

where $0.5 \times radnet_{veg}$ is the daily average of net radiation at vegetation when daily change of radiation was approximated by \sin^2 . The constant 1012 is the specific heat of air (in $J \text{ kg}^{-1} \text{ K}^{-1}$), 695 is the latent heat of vaporization (in $Wh \text{ kg}^{-1} \text{ H}_2\text{O}$), and 0.667 is the psychrometer constant (in hPa K^{-1}); c_{aero} , c_{soil} , and c_{leaf} are aerodynamic conductance, soil surface conductance, and canopy conductance, respectively; c_{aero} , aerodynamic conductance is proportional to wind velocity:

$$c_{aero} = \frac{1.0 + 0.537 \times wind}{250.1} . \quad (A46)$$

This equation was delivered by substituting empirical formulation of Penman (1948) into equation A44. c_{soil} , soil surface conductance, is in proportion to the fraction of soil layer 1 that is saturated with water:

$$c_{soil} = 0.0015 \times \min \left[\left(\frac{pool_{w(1)}}{Wfi \times Depth_{(1)}} \right)^2, 1 \right], \quad (A47)$$

where the multiplier 0.002 is water-saturation conductance., which is a tuning parameter
Finally, c_{leaf} is

$$c_{leaf} = 0.0224 \times ccon , \quad (A48)$$

where the multiplier 0.0224 is the unit converter from $[\text{mol H}_2\text{O m}^{-2} \text{s}^{-1}]$ to $[\text{m}^3 \text{H}_2\text{O m}^{-2} \text{s}^{-1}]$.

Due to the limited water availability, evapotranspiration rates were reduced from their potential values, ev_{pm} and tr_{pm} , to their actual values, ev and tr , as approximated by the quadratic functions:

$$0.1 ev^2 - (a + ev_{pm}) ev + a \times ev_{pm} = 0, \quad (A49)$$

$$0.1 \, tr^2 - (b + tr_{pm}) \, tr + b \times tr_{pm} = 0, \quad (A50)$$

where 0.1 is the empirical convexity of the available water to the actual evapotranspiration curves; a and b are available water for evaporation and transpiration, respectively; $a = pool_{w(1)}$, $b = \max(0, pool_{w(1)} - Depth_{(1)} \times Wwilt) + \max(0, pool_{w(2)} - Depth_{(2)} \times Wwilt)$. These equations can be transformed as follows:

$$ev = \frac{(a + ev_{pm}) - \sqrt{(a + ev_{pm})^2 - 4 \times 0.1 \times a \times ev_{pm}}}{2 \times 0.1}, \quad (A51)$$

$$tr = \frac{(b + tr_{pm}) - \sqrt{(b + tr_{pm})^2 - 4 \times 0.1 \times b \times tr_{pm}}}{2 \times 0.1}, \quad (A52)$$

Actual evaporation, ev , is charged only for soil layer 1. Actual transpiration, tr , is charged for soil layers 1 and 2 in proportion to the soil wetness of each layer.

1 **Appendix B**

2 B1. Inputs and outputs of the SEIB–DGVM

3 **Input**

4 (1) Location

5 latitude, altitude

6 (2) Soil (fixed in time)

7 soil moisture at saturation point, field capacity, matrix potential, wilting point, albedo

8 (3) Climatic data (daily)

9 air temperature, soil temperature, fraction of cloud cover, precipitation, humidity, wind

10 velocity

11 **Outputs**

12 (1) Carbon dynamics (daily–yearly)

13 terrestrial carbon pool (woody biomass, grass biomass, litter, soil organic matter), CO₂

14 absorption and emission rates

15 (2) Water dynamics (daily)

16 soil moisture content (three layers), interception rate, evaporation rate, transpiration rate,

17 interception rate, runoff rate

- 1 (3) Radiation (daily)
- 2 albedo from terrestrial surface
- 3 (4) Properties of vegetation (daily–yearly)
- 4 vegetation type, dominant plant functional type, leaf area index, tree density, size distribution
- 5 of trees, age distribution of trees, woody biomass for each tree, grass biomass per unit area

1 B2. Processes in the SEIB–DGVM, and the approaches used to represent each process

Process	Approach	Source
<i>Physical process</i>		
Radiation	Beer's Law within spatially explicit virtual forest	
Evapotranspiration	Penman–Monteith evapotranspiration	Monteith and Unsworth (1990)
Soil water process	Empirical analogs of Darcy's law: saturated and unsaturated percolation in three soil layers	Neilson (1995)
<i>Physiology</i>		
Photosynthesis	Michaelis-type function	
Maintenance respiration	The respiration rate is in proportion to the nitrate content of each organ.	Ryan (1991)
Growth respiration	The respiration rate is based on the chemical composition of each organ.	Poorter (1994)
Stomatal conductance	A semiempirical model	Ball et al. (1987) modified by Leuning (1995)
Phenology	A set of semiempirical models; parameters were estimated from satellite NDVI data.	Botta et al. (2000)
Decomposition	Three carbon sources: litter and soil organic carbon with slow and fast decomposition rates	Foley (1995) and Lloyd and Taylor (1994)
<i>Vegetation dynamics</i>		
Establishment	Climatically favored PFTs establish as small individuals.	
Mortality	Annual NPP per leaf area, heat stress, bioclimatic limit, and fire	Sitch et al. (2003)
Disturbance	Fire as an empirical function of soil moisture and aboveground biomass	Kistler et al. (2001)

B3. Parameters and constants in the model's equations

2 Fixed parameters (begins with a capital letter)

3 Soil properties (Grid specific)

4 W_{sat} : soil moisture at saturation point (m m^{-1})

5 W_{fi} : soil moisture at field capacity (m m^{-1})

6 W_{mat} : soil moisture at matrix potential (m m^{-1})

7 W_{wilt} : soil moisture at wilting point (m m^{-1})

8 $ALBEDO$: soil albedo (fraction)

9 $Depth_{(n)}$: depth of soil layer n (mm)

10

11 Soil properties (Global value)

12 $K_{u1(n)}, K_{u2(n)}$: percolation coefficients of unsaturated soil of soil layer n (dimensionless)

13 $K_{s1(n)}, K_{s2(n)}$: percolation coefficients of saturated soil of soil layer n (dimensionless)

14

15 Location

16 LAT : latitude (degree)

17 ALT : altitude (m)

18

19 Allocation and Allometry (PFT-specific)

20 $HGTmax$: maximum tree height (m)

21 $HGTs$: initial value of relative growth rate, height to diameter (m m^{-1})

22 LAm_{ax} : maximum leaf area per canopy surface ($\text{m}^2 \text{m}^{-2}$)

1	CD_{max}	: maximum crown diameter (m)
2	SLA	: specific leaf area (one sided $m^2 g DM^{-1}$)
3	$ALM_{1, 2}$: allometric parameter 1, 2 (dimensionless)
4	ALM_3	: allometric parameter 3 ($g DM m^{-3}$)
5	$ALM_{4, 5, 6}$: allometric parameter 4, 5, 6 (fraction)
6	$FRratio$: ratio of foliage mass to fine root mass (ratio)
7		
8	Respiration and turnover (PFT-specific)	
9	$PN_{f, s, r}$:nitrogen mass per biomass for foliage, sapwood, root ($g N g DM^{-1}$)
10	RM	:maintenance respiration rate at 15°C for unit nitrogen mass ($g C g N^{-1} day^{-1}$)
11	$RG_{f, s, r}$:specific growth respiration rate for foliage, sapwood, and root ($g DM g DM^{-1}$)
12	$RG_{stockin}$:growth respiration rate from available resource to stock resource ($g DM g$
13		DM^{-1})
14	$RG_{stockout}$:growth respiration rate from stock resource to available resource ($g DM g$
15		DM^{-1})
16	$TO_{f, s, r}$:turnover rate for foliage, sapwood, and root ($DM^{-1} year^{-1}$)
17	$TO_{fast, slow}$:turnover rates for fast and slow soil organic matter (SOM) ($DM^{-1} yr^{-1}$)
18		
19	Photosynthesis (PFT-specific)	
20	P_{MAX}	: maximum photosynthesis rate ($\mu mol CO_2 m^{-2} s^{-1}$)
21	EK	: light attenuation coefficient for vertical direction (dimensionless)
22	LUE	: control value of light-use efficiency for photosynthesis ($mol CO_2 mol photon^{-1}$)
23	T_{opt0}	:optimum temperature for photosynthesis at very low intercellular CO_2
24		concentration ($^{\circ}C$)

1	T_{min}	: minimum temperature for photosynthesis (°C)
2	T_{max}	: maximum temperature for photosynthesis (°C)
3	GS_{b1}	: parameters for stomatal conductance (mol H ₂ O m ⁻² s ⁻¹)
4	GS_{b2}	: parameters for stomatal conductance (dimensionless)
5	GS_{b3}	: parameters for stomatal conductance (hPa)
6	KM	: dependence of photosynthesis on intercellular CO ₂ concentration (μmol mol ⁻¹)
7	$CO2_{cmp}$: CO ₂ compensation point at 20°C (μmol CO ₂ mol ⁻¹ air)
8		
9	Establishment (PFT-specific)	
10	$P_{establish}$: establishment probability at vacant patch (m ⁻² year ⁻¹)
11	GDD_{min}	: minimum growth-degree-day sum (5 °C base)
12	TC_{max}	: maximum coldest-month temperature (°C)
13		
14	Mortality (PFT-specific)	
15	M_1	: parameter for background mortality (dimensionless)
16	M_2	: parameter for background mortality (dimensionless)
17	M_3	: probability of survival after fire (varying 0.0–1.0)
18	TC_{min}	: minimum coldest-month temperature for survival (°C)
19		
20	Other fixed parameters	
21	ESD	: distance between sun and earth (km)
22	ESD_{mean}	: annual mean of ESD (km)
23		

1 **Variables (Begins with a lowercase letter)**

2 **Daily climatic data**

- 3 *tmp_{air}* : air temperature (°C)
4 *tmp_{soil}* : soil temperature at 10 cm depth (°C)
5 *cloud* : total cloud cover (fraction)
6 *prec* : daily precipitation (mm day⁻¹)
7 *humid* : air humidity (g g⁻¹)
8 *wind* : wind velocity (m s⁻¹)

9

10 **Woody biomass (for each individual tree)**

- 11 *mass_{leaf}* : leaf biomass (g DM)
12 *mass_{trunk}* : trunk biomass (g DM)
13 *mass_{root}* : fine root biomass (g DM)
14 *mass_{stock}* : stock biomass (g DM)
15 *mass_{available}* : available biomass (g DM)

16

17 **Grass biomass**

- 18 *gmass_{leaf}* : leaf biomass density of grass (g DM m⁻²)
19 *gmass_{root}* : root biomass density of grass (g DM m⁻²)
20 *gmass_{stock}* : stock biomass density of grass (g DM m⁻²)
21 *gmass_{available}* : available biomass density of grass (g DM m⁻²)

22

23 **Morphology and characteristics for woody PFTs (for each individual tree)**

- 24 *height* : tree height (m)

1	$crown_{diameter}$: crown diameter (m)
2	$crown_{depth}$: crown depth (m)
3	$crown_{area}$: cross sectional crown area (m ²)
4	$dbh_{sapwood}$: sapwood diameter (m)
5	$dbh_{heartwood}$: heartwood diameter (m)
6	la	: leaf area (m ²)
7	la_{mean}	: annual mean leaf area in the previous year (m ²)
8		
9	Photosynthesis conditions	
10	p_{ave}	: daily average of photosynthetic rates for each woody individual (μmol
11		CO ₂ m ⁻² s ⁻¹)
12	p_{sat}	: light saturated photosynthetic rate (μCO ₂ m ⁻² s ⁻¹)
13	lue	: light-use efficiency of photosynthesis (mol CO ₂ mol photon ⁻¹)
14	$co2_{cmp}$: CO ₂ compensation point (μmol CO ₂ mol air ⁻¹)
15	$co2_{cell}$: intercellular CO ₂ concentration (μmol CO ₂ mol air ⁻¹)
16	t_{opt}	: optimum temperature for photosynthesis (°C)
17	gs	: midday leaf stomatal conductance of H ₂ O (mol H ₂ O m ⁻² s ⁻¹)
18	gs_{top}	: midday leaf stomatal conductance of H ₂ O on top of the leaf-layer (mol
19		H ₂ O m ⁻² s ⁻¹)
20	$ccon_{wood}$: stomatal conductance of H ₂ O of tree canopy, day time mean (mol H ₂ O
21		m ⁻² s ⁻¹)
22	$ccon_{grass}$: stomatal conductance of H ₂ O of grass leaves, day time mean (mol H ₂ O
23		m ⁻² s ⁻¹)
24	$ccon$: stomatal conductance of H ₂ O, day time mean (=ccon _{wood} + ccon _{grass} , mol

1		$\text{H}_2\text{O m}^{-2} \text{ s}^{-1}$)
2		
3	Production	
4	gpp	: gross primary production of each tree (g DM day^{-1})
5	gpp_l	: gross primary production of each crown layer (g DM day^{-1})
6	gpp_g	: gross primary production of grass layer ($\text{g DM day}^{-1} \text{ m}^{-2}$)
7	$anpp$: annul net primary production of the previous year (kg DM year^{-1})
8	$stat_{leaf}$: benefit per cost of maintaining leaf mass ($\text{g g}^{-1} \text{ day}^{-1}$)
9		
10	Other metabolic variables	
11	lai	: leaf area index of each PFT ($\text{m}^2 \text{ m}^{-2}$)
12	lai_g	: leaf area index of grass layer ($\text{m}^2 \text{ m}^{-2}$)
13	$stat_{water}$: state of water availability for each PFT (varying 0.0–1.0)
14	qt	: temperature sensitivity of respiration (dimensionless)
15		
16	Soil water cycle	
17	$prec_{rain}$: precipitation, rain (mm day^{-1})
18	$prec_{snow}$: precipitation, snow (mm day^{-1})
19	$rain$: expected number of rain in a day (day^{-1})
20	$pool_{w(n)}$: water content at soil layer n (mm)
21	$pool_{snow}$: water-equivalent snow depth (mm)
22	tw	: snowmelt rate (mm day^{-1})
23	$pn_{(n)}$: penetration rate for soil layer n (mm day^{-1})
24	ev	: actual evaporation rate from soil layer 1 (mm day^{-1})

1	ev_{pm}	: potential evaporation rate from soil layer 1 (mm day^{-1})
2	$tr_{(n)}$: actual transpiration rate from soil layer n (mm day^{-1})
3	tr_{pm}	: potential transpiration rate (mm day^{-1})
4	ic	: intercepted rainfall by plants (mm day^{-1})
5	aet	: actual evapotranspiration of the previous year (mm year^{-1})
6	c_{aero}	: aerodynamic conductance of evaporation (dimensionless)
7	c_{soil}	: soil conductance of evapotranspiration (dimensionless)
8	c_{leaf}	: canopy conductance of transpiration (dimensionless)
9		
10	Radiation conditions at midday	
11	rad_{intact}	: shortwave radiation at top of atmosphere (W m^{-2})
12	rad	: shortwave radiation entering biosphere (W m^{-2})
13	rad_{direct}	: direct radiation within rad (W m^{-2})
14	$rad_{diffuse}$: diffused radiation within rad (W m^{-2})
15	$radnet_{veg}$: net radiation at vegetation surface (W m^{-2})
16	$radnet_{soil}$: net radiation at soil surface (W m^{-2})
17	$radnet_{long}$: net long wave radiation (W m^{-2})
18	par	: midday PAR ($\mu\text{mol photon m}^{-2} \text{s}^{-1}$)
19	par_{direct}	: direct radiation component of par ($\mu\text{mol photon m}^{-2} \text{s}^{-1}$)
20	$par_{diffuse}$: diffused radiation component of par ($\mu\text{mol photon m}^{-2} \text{s}^{-1}$)
21	$par_{wood(l, n)}$: midday PAR on crown layer l of individual tree n ($\mu\text{mol photon m}^{-2} \text{s}^{-1}$)
22	par_{grass}	: midday PAR at the grass layer ($\mu\text{mol photon m}^{-2} \text{s}^{-1}$)
23	$fpar_{direct(l, n)}$: relative intensity of direct PAR of crown disk l of tree n at midday
24		compared to the forest top (dimensionless)

1	$fpar_{diffuse(l)}$: relative intensity of diffused of forest layer l at midday compared to the
2		forest top (dimensionless)
3	$fpar_{direct}$: relative intensity of direct PAR of crown disk l of tree n at midday
4		compared to the forest top (dimensionless)
5	sl_{hgt}	: solar angle at midday (degree)
6	sl_{dec}	: solar declination of the Earth's orbit (degree)
7	$dlen$: day length (hour)
8	eK	: light attenuation coefficient at midday (dimensionless)
9	ir	: shortwave interception by leaves (fraction)
10	$albedo_{veg}$: albedo of vegetation surface (fraction)
11	$albedo_{soil}$: albedo of soil surface (fraction)
12		
13	Air characteristics	
14	ap	: air pressure (hPa)
15	vp	: actual vapor pressure (hPa)
16	vp_{sat}	: saturated vapor pressure (hPa)
17	vpd	: vapor pressure deficit between saturated and actual vapor pressures (hPa)
18	$co2atm$: ambient (canopy) CO ₂ concentration ($\mu\text{mol CO}_2 \text{ mol}^{-1} \text{ air}$)
19	$slope_{vps}$: slope of saturated vapor pressure ($\text{hPa } ^\circ\text{C}^{-1}$)
20	dn_{sa}	: density of air (kg m^{-3})

B4. PFT-specific allocation and allometric parameters

PFT	ALM_1	ALM_2	ALM_3	ALM_4	ALM_5	ALM_6	HGT_{max}	$HGTs$	$FRratio$	SLA	LAm_{max}	CD_{max}
	-	-	(g DM m ⁻³)	(ratio)	(ratio)	(ratio)	(m)	(m m ⁻¹)	(ratio)	(m ² g ⁻¹)	(m ² m ⁻²)	(m)
TrBE 1	-	-	62000 0	-	0.3	0.37	68.0	140.0	1.90	0.010	2.0	30.0
TrBE 2	-	-	57000 0	-	0.3	0.28	68.0	100.0	1.90	0.010	2.0	30.0
TrBE 3	-	-	37000 0	-	0.3	0.28	54.0	95.0	1.90	0.010	2.0	30.0
TrBE 4	-	-	71000 0	-	0.3	0.28	42.0	95.0	1.90	0.010	2.0	30.0
TrBR	7000	200	49200 0	0.50	-	-	35.0	150.0	1.50	0.013	5.0	15.0
TeNE	4800	100	37400 0	0.38	-	-	43.0	65.0	1.50	0.004	4.0	15.0
TeBE	4800	200	49200 0	0.38	-	-	17.0	154.3	1.50	0.007	4.0	15.0
TeBS	14500	200	49200 0	0.20	-	-	37.0	159.0	1.50	0.015	2.0	15.0
BoNE	6000	100	37400 0	0.20	-	-	35.0	130.0	1.50	0.004	2.0	10.0
BoNS	6000	-	-	-	-	-	31.7	165	0.17	0.014	4.0	8.0
BoBS	8500	200	49200 0	0.30	-	-	35.0	200.0	1.50	0.016	4.0	10.0
TeH	-	-	-	-	-	-	-	-	1.00	0.020	-	-
TrH	-	-	-	-	-	-	-	-	1.00	0.015	-	-

1

B5. PFT-specific dynamic parameters

PFT	M_1 (no dimension)	M_2 (no dimension)	M_3 (no dimension)	$P_{establish}$ (m ⁻² year ⁻¹)	TC_{min} (°C)	TC_{max} (°C)	GDD_{min} (5 °C base)
TrBE	0.015	1.5	0.12	0.015	15.5	-	-
TrBR	0.015	1.5	0.50	0.015	15.5	-	-
TeNE	0.018	1.0	0.12	0.040	-2.0	22.0	900
TeBE	0.018	1.0	0.50	0.040	3.0	18.8	1200
TeBS	0.010	2.5	0.12	0.013	-17.0	15.5	1200
BoNE	0.013	1.2	0.12	0.005	-32.5	-2.0	600
BoNS	0.007	2.0	-	0.010	-	-2.0	350
BoBS	0.015	2.0	0.12	0.020	-	-2.0	350

2

1

B6. PFT-specific respiration and turnover parameters

PFT	RM	PN_f	RG_f	RG_s	RG_r	$RG_{stockin}$	$RG_{stockout}$	TO_f	TO_s	TO_r
	(gC gN ⁻¹ day ⁻¹)	(gN gDM ⁻¹)	(gDM gDM ⁻¹)	(gDM gDM ⁻¹)	(gDM gDM ⁻¹)	(gDM gDM ⁻¹)	(gDM gDM ⁻¹)	(year ⁻¹)	(year ⁻¹)	(year ⁻¹)
TrBE	0.1	0.016	1.56	1.68	1.34	1.10	1.10	0.59	0.05	0.76
TrBR	0.1	0.022	1.56	1.68	1.34	1.10	1.10	1.59	0.05	0.76
TeNE	0.1	0.012	1.56	1.68	1.34	1.10	1.10	0.22	0.05	0.64
TeBE	0.1	0.012	1.56	1.68	1.34	1.10	1.10	0.38	0.05	0.64
TeBS	0.1	0.022	1.56	1.68	1.34	1.10	1.10	2.17	0.05	0.64
BoNE	0.1	0.012	1.56	1.68	1.34	1.10	1.10	0.22	0.05	0.42
BoNS	0.1	0.026	1.35	1.68	1.11	1.10	1.10	4.00	0.05	0.16
BoBS	0.1	0.025	1.56	1.68	1.34	1.10	1.10	3.33	0.05	0.42
TeH	0.1	0.027	1.50	-	1.34	1.10	1.10	3.19	-	0.40
TrH	0.1	0.018	1.50	-	1.34	1.10	1.10	6.70	-	0.90

2

1

B7. PFT-specific photosynthesis parameters

PFT	P_{MAX} ($\mu\text{mol CO}_2$ m^{-2} s^{-1})	EK no dimension	LUE (mol CO_2 mol photon^{-1})	T_{opt0} ($^{\circ}\text{C}$)	T_{min} ($^{\circ}\text{C}$)	T_{max} ($^{\circ}\text{C}$)	GS_{b1} ($\text{mol H}_2\text{O}$ m^{-2} s^{-1})	GS_{b2} no dimension	GS_{b3} (hPa)	KM ($\mu\text{mol mol}^{-1}$)	$CO2_{cmp}$ ($\mu\text{mol CO}_2$ mol^{-1} air)
TrBE	14.0	0.50	0.05	27.5	2.0	47.5	0.01	5.0	10.0	33.0	50.0
TrBR	14.0	0.50	0.05	27.5	2.0	47.5	0.01	5.0	10.0	30.0	50.0
TeNE	9.0	0.50	0.05	25.0	0.0	45.0	0.01	5.0	10.0	30.0	50.0
TeBE	9.0	0.50	0.05	25.0	0.0	45.0	0.01	5.0	10.0	30.0	50.0
TeBS	12.0	0.50	0.05	22.5	-2.0	42.5	0.01	5.0	10.0	30.0	50.0
BoNE	9.3	0.50	0.05	18.0	-4.0	38.5	0.01	5.0	10.0	30.0	50.0
BoNS	11.0	0.50	0.05	20.0	-2.0	35.0	0.01	10.0	10.0	30.0	50.0
BoBS	9.0	0.50	0.05	18.0	-4.0	38.5	0.01	5.0	10.0	35.0	50.0
TeH	11.0	0.50	0.05	-	-1.0	45.0	0.01	5.0	10.0	37.0	50.0
TrH	18.0	0.50	0.05	-	2.5	55.0	0.01	2.0	10.0	10.0	5.0

2

1

B8. Soil percolation parameters for each soil layer (dimensionless)

Soil layer	K_{1u}	K_{2u}	K_{1s}	K_{2s}
1	0.80	2.5	0.30	2.0
2	0.15	3.0	0.30	3.0
3	0.01	10.0	0.30	10.0

2

1 B9. Classification scheme of vegetation type, taken from Haxeltine and Prentice (1996) with
2 some simplifications.

Vegetation type conditions	Dominant PFT	Other
Group 1		
Desert (polar)	any	$GDD_0 < 150$
Group 2		
Arctic / Alpine-tundra	any	$GDD_5 < 350$
Group 3		
Tropical forest	TrBE	$2.5 \leq LAI_{max}$
Tropical deciduous forest	TrBR	$2.5 \leq LAI_{max}$
Temperate evergreen forest	TeNE	$1.5 \leq LAI_{max}$
Temperate evergreen forest	TeBE	$3.0 \leq LAI_{max}$
Temperate deciduous forest	TeBS	$2.5 \leq LAI_{max}$
Boreal evergreen forest	BoNE	
Boreal deciduous forest	BoNS or BoBS	
Group 4		
Xeric wood-land / scrub	Tropical woody or TeBE	$1.0 \leq LAI_{max}$
	Boreal woody or TeNE or TeBS	$1.5 \leq LAI_{max}$
Group 5		
Grass land / Savannas / Steppe	any	$0.2 \leq LAI_{max}$
Desert (arid)	any	$LAI_{max} < 0.2$

3 Priority of classification: Group 1 > Group 2 > Group 3 > Group 4 > Group 5

4 GDD_0 : growing-degree-day at 0 °C base

5 GDD_5 : growing-degree-day at 5 °C base

6 LAI_{max} : maximum leaf area index of the previous year ($m^2 m^{-2}$)

Literature cited

- 2 Arora, V., 2002. Modeling vegetation as a dynamic component in soil-vegetation-atmosphere
3 transfer schemes and hydrological models. *Rev. Geophys.* 40, 1006,
4 doi:10.1029/2001RG000103.
- 5 Arora, V.K., Boer, G.J., 2005. A parameterization of leaf phenology for the terrestrial
6 ecosystem component of climate models. *Global Change Biol.* 11, 39–59.
- 7 Ball, J.T., Woodrow, I.E., Berry, J.A., 1987. A model predicting stomatal conductance and its
8 contribution to the control of photosynthesis under different environmental conditions. In:
9 Biggens, J. (Eds.), *Progress in Photosynthesis Research*. Martinus Nijhoff Publishers,
10 Dordrecht, pp. 221–224.
- 11 Botta, A., Viovy, N., Ciais, P., Friedlingstein, P., Monfray, P., 2000. A global prognostic
12 scheme of leaf onset using satellite. *Global Change Biol.* 6, 709–725.
- 13 Brooks, A., Farquhar, G.D., 1985. Effect of temperature on the CO₂/O₂ specificity of ribulose
14 1,5-bisphosphate carboxylase/oxygenase and the rate of respiration in the light, Estimates
15 from gas-exchange measurements on spinach. *Planta* 165, 397–406.
- 16 Bugmann, H., 2001. A review of forest gap models. *Clim. Change* 51, 259–305.
- 17 Cox, P.M., 2001. Description of the "TRIFFID" Dynamic GLobal Vegetation Model. Hadley
18 Centre technical note 24, 1–16.
- 19 Cox, P.M., Betts, R.A., Jones, C.D., Spall, S.A., Totterdell, I.J., 2000. Acceleration of global
20 warming due to carbon-cycle feedbacks in a coupled climate model. *Nature* 408, 184–187.
- 21 Cramer, W., Bondeau, A., Woodward, F.I., Prentice, I.C., Betts, R.A., Brovkin, V., Cox, P.M.,
22 Fisher, V., Foley, J.A., Friend, A.D., Kucharik, C., Lomas, M.R., Ramankutty, N., Sitch, S.,
23 Smith, B., White, A., Young-Molling, C., 2001. Global response of terrestrial ecosystem
24 structure and function to CO₂ and climate change: results from six dynamic global vegetation
25 models. *Global Change Biol* 7, 357–373.
- 26 Farquhar, G.D., von Caemmerer, S., 1982. Modelling of photosynthetic response to
27 environmental conditions. In: Nobel, P.S., Osmond, C.B., Ziegler, H. (Eds.), *Physiological*
28 *Plant Ecology II: Water Relations and Carbon Assimilation*. Springer, Berlin, pp. 549–587.
- 29 Farquhar, G.D., von Caemmerer, S., Berry J.A., 1980. A biochemical model of photosynthetic
30 CO₂ assimilation in leaves of C3 plants. *Planta* 149, 78–90.
- 31 FFPRI (Forestry and Forest Products Research Institute), 1982. Properties of timber. In: *The*
32 *handbook of wood industries*, 3rd eds (in Japanese). Maruzen Publishers, Tokyo, pp. 62–63.
- 33 FFPRI (Forestry and Forest Products Research Institute), Viewed October 27 2004, 2003.
34 Forest Dynamics Database (<http://fddb.ffpri-108.affrc.go.jp/>).
- 35 Foley, J.A., 1995. An equilibrium model of the terrestrial carbon budget. *Tellus, Ser. B* 47,

1 310–319.

2 Foley, J.A., Costa, M.H., Delire, C., Ramankutty, N., Snyder, P., 2003. Green surprise? How
3 terrestrial ecosystems could affect earth's climate. *Frontier Ecol. Environ.* 1, 38–44.

4 Friend, A.D., Stevens, A.K., Knox, R.G., Cannell, M.G.R., 1997. A process-based, terrestrial
5 biosphere model of ecosystem dynamics (Hybrid v3.0). *Ecol. Modell.* 95, 249–287.

6 Gill, R.A., Jackson, R.B., 2000. Global patterns of root turnover for terrestrial ecosystems.
7 *New Phytol.* 147, 13–31.

8 Greene, D.F., Zasada, J.C., Sirois, L., Kneeshaw, D., Morin, H., Charron, I., Simard, M.-J.,
9 1999. A review of the regeneration dynamics of North American boreal forest tree species.
10 *Can. J. For. Res.* 29, 824–839.

11 Haxeltine, A., Prentice, I.C., 1996. BIOME3: An equilibrium terrestrial biosphere model
12 based on ecophysiological constraints, resource availability, and competition among plant
13 functional types. *Global Biogeochem. Cycles* 10, 693–709.

14 Hillel, D., 1982. *Introduction to soil physics*. Academic Press, New York, USA.

15 Ito, A., Oikawa, T., 2002. A simulation model of the carbon cycle in land ecosystems
16 (Sim-CYCLE): a description based on dry-matter production theory and plot-scale validation.
17 *Ecol. Modell.* 151, 143–176.

18 Joos, F., Prentice, I.C., Sitch, S., Meyer, R., Hooss, G., Plattner, G., Gerber, S., Hasselmann,
19 K., 2001. Global warming feedbacks on terrestrial carbon uptake under the Intergovernmental
20 Panel on Climate Change (IPCC) emission scenarios. *Global Biogeochem. Cycles* 15,
21 891–907.

22 Jones, H. G., 1992. Radiation. In: *Plants and microclimate*, 2nd ed, pp:9–44, Cambridge
23 University press.

24 Kira, T., Shidei, T., 1967. Primary production and turnover of organic matter in different
25 forest ecosystems of the western Pacific. *Jpn. J. Ecol.* 17, 70–87.

26 Kistler, R., Kalnay, E., Collins, W., Saha, S., White, G., Woollen, J., Chelliah, M., Ebisuzaki,
27 W., Kanamitsu, M., Kousky, V., van den Dool, H., Jenne, R., Fiorino, M., 2001. The
28 NCEP-NCAR 50-year reanalysis: monthly means CD-ROM and documentation. *Bull. Am.*
29 *Meteorol. Soc.* 82, 247–267.

30 Kohyama, T., Shigesada, N., 1995. A size-distribution-based model of forest dynamics along a
31 latitudinal environmental gradient. *Vegetatio* 121, 117–126.

32 Kohyama, T., Suzuki, E., Aiba, S., Seino, T., 1999. Functional differentiation and positive
33 feedback enhancing plant biodiversity. In: Kato, M. (Eds.), *Biology of Biodiversity*. Springer,
34 Tokyo, pp. 179–191.

35 Kohyama, T., 2005. Scaling up from shifting-gap mosaic to geographic distribution in the
36 modeling of forest dynamics. *Ecol. Res.* 20, 305–312.

37 Köppen, W., 1936. *Das Geographische System der Klimate*. In: Köppen, W. and Geiger, R.
38 (Eds.), *Handbuch der Klimatologie*. Gebruder Borntraeger, Berlin, pp. C1–C44.

- 1 Krinner, G., Viovy, N., de Noblet-Ducoudre, N., Ogee, J., Polcher, J., Friedlingstein, P., Ciais,
2 P., Sitch, S., Prentice, I.C., 2005. A dynamic global vegetation model for studies of the
3 coupled atmosphere-biosphere system. *Global Biogeochemical Cycles* 19, GB1015.
- 4 Kucharik, C.J., Foley, J.A., Delire, C., Fisher, V.A., Coe, M.T., Lenters, J.D., Young-Molling,
5 C., Ramankutty, N., Norman, J.M., Gower, S.T., 2000. Testing the performance of a Dynamic
6 Global Ecosystem Model: Water balance, carbon balance, and vegetation structure. *Global*
7 *Biogeochemical Cycles* 14, 795–825.
- 8 Kuroiwa, S., 1979. Population photosynthesis. In: Iwajyo, H. (Eds.), *Function and*
9 *productivity of plant population (in Japanese)*. Asakura-shoten, Tokyo, pp. 84–141.
- 10 Lambers, H., Chapin III, F.S., Pons, T.L., 1998. *Plant Physiological Ecology*. Springer,
11 New-York.
- 12 Larcher, W., 1995. Ecophysiology and stress physiology of functional groups. In: *Physical*
13 *plant ecology*. Springer, Berlin, p. 506.
- 14 Leuning, R., 1995. A critical appraisal of a combined stomatal-photosynthesis model for C₃
15 plants. *Plant Cell Environ.* 18, 339–355.
- 16 Lloyd, J., Taylor, J.A., 1994. On the temperature dependence of soil respiration. *Func. Ecol.* 8,
17 315–323.
- 18 Monteith, J.L., Unsworth, M.H., 1990. *Principles of Environmental Physics*. 2nd edition.
19 Arnold Press, London.
- 20 Neilson, R.P., 1995. A model for predicting continental-scale vegetation distribution and water
21 balance. *Ecol. Appl.* 5, 362–385.
- 22 Osmond, C.B., Björkman, O., Anderson, D.J., 1980. Photosynthesis. In: *Physiological*
23 *Processes in Plant Ecology*. Springer-Verlag, Berlin, pp. 291–377.
- 24 Pacala, S.W., Deutschman, D.H., 1995. Details that matter: The spatial distribution of
25 individual trees maintains forest ecosystem function. *Oikos* 74, 357–365.
- 26 Peng, C.H., 2000. From static biogeographical model to dynamic global vegetation model: a
27 global perspective on modelling vegetation dynamics. *Ecol. Modell.* 135, 33–54.
- 28 Penman, H.L., 1948. Natural evaporation from open water, bare soil and grass. *Proc. Roy. Soc.*
29 *London, A* 193.
- 30 Penning de Vries, F.W.T., 1975. Use of assimilates in higher plants. In: Cooper, J.P. (Eds.),
31 *Photosynthesis and productivity in different environments*. Cambridge Univ. Press, pp.
32 459–480.
- 33 Pitman, A.J., 2003. The evolution of, and revolution in, land surface schemes designed for
34 climate models. *International Journal of Climatology* 23, 479–510.
- 35 Poorter, H., 1994. Construction costs and payback time of biomass: A whole plant perspective.
36 In: Roy, J., Garnier, E. (Eds.), *A whole plant perspective on carbon-nitrogen interactions*. SPB
37 Academic Publishing, Hague, Netherlands, pp. 111–127.

- 1 Pregitzer, K.S., Euskirchen, E.S., 2004. Carbon cycling and storage in world forests: biome
2 patterns related to forest age. *Global Change Biol.* 10, 2052–2077.
- 3 Raich, J.W., Rastetter, E.B., Melillo, J.M., Kicklighter, D.W., Steudler, P.A., Peterson, B.J.,
4 Grace, A.L., Moore III, B., Vörösmarty, C.J., 1991. Potential net primary productivity in
5 South America: application of a global model. *Ecol. Appl.* 1, 399–429.
- 6 Reich, P.B., Walters, M.B., Ellsworth, D.S., 1997. From tropics to tundra: Global convergence
7 in plant functioning. *Proc. Natl. Acad. Sci. USA* 94, 13730–13734.
- 8 Ryan, M.G., 1991. Effects of climate change on plant respiration. *Ecol. Appl.* 1, 157–167.
- 9 Sala, O.E., 2001, Productivity of temperate grasslands. In: Roy, J., Saugier, B., Mooney, H.A.
10 (Eds.), *Terrestrial Global Productivity*. Academic Press, pp. 285–300.
- 11 Schulze, E.-D., Schulze, W., Kelliher, F.M., Vygodskaya, N.N., Ziegler, W., Kobak, K.I.,
12 Koch, H., Arneth, A., Kusnetsova, W.A., Sogatchev, A., Issajev, A., Bauer, G., Hollinger, D.Y.,
13 1995. Aboveground biomass and nitrogen nutrition in a chronosequence of pristine Dahurian
14 *Larix* stands in eastern Siberia. *Can. J. For. Res.* 25, 943–960.
- 15 Shinozaki, K., Yoda, K., Hozumi, K., Kira, T., 1964a. A quantitative analysis of plant form —
16 The pipe model theory I. *Jpn. J. Ecol.* 14, 97–105.
- 17 Shinozaki, K., Yoda, K., Hozumi, K., Kira, T., 1964b. A quantitative analysis of plant form —
18 The pipe model theory II: Further evidence of the theory and its application in forest ecology,
19 *Jpn. J. Ecol.* 14, 133–139.
- 20 Sitch, S., Smith, B., Prentice, I.C., Arneth, A., Bondeau, A., Cramer, W., Kaplan, J.O., Levis,
21 S., Lucht, W., Sykes, M.T., Thonicke, K., Venevski, S., 2003. Evaluation of ecosystem
22 dynamics, plant geography and terrestrial carbon cycling in the LPJ dynamic global
23 vegetation model. *Global Change Biol.* 9, 161–185.
- 24 Smith, B., Prentice, I.C., Sykes, M.T., 2001. Representation of vegetation dynamics in the
25 modelling of terrestrial ecosystems: comparing two contrasting approaches within European
26 climate space. *Global Ecology and Biogeography* 10, 621–637.
- 27 Starfield, A.M., Chapin III, F.S., 1996. Model of transient changes in arctic and boreal
28 vegetation in response to climate and land use change. *Ecol. Appl.* 6, 842–864.
- 29 Takahashi, K., Homma, K., Vetrova, V.P., Florenzev, S., Hara, T., 2001. Stand structure and
30 regeneration in a Kamchatka mixed boreal forest. *Journal of vegetation science* 12, 627–634.
- 31 Takenaka, A., 2005. Local coexistence of tree species and the dynamics of global distribution
32 pattern along an environmental gradient: a simulation study. *Ecol. Res.* 20, 297–304.
- 33 Thonicke, K., Venevsky, S., Sitch, S., Cramer, W., 2001. The role of fire disturbance for
34 global vegetation dynamics: coupling fire into a Dynamic Global Vegetation Model. *Global*
35 *Ecology and Biogeography* 10, 661–677.
- 36 Waring, R.H., 1983. Estimating forest growth and efficiency in relation to canopy leaf area.
37 *Adv. Ecol. Res.* 13, 327–354.
- 38 Woodward, F.I., Lomas, M.R., 2004. Vegetation dynamics – simulating responses to climatic

- 1 change. Biol. Rev. 79, 643–670.
- 2 Woodward, F.I., Lomas, M.R., Betts, R.A., 1998. Vegetation-climate feedbacks in a
3 greenhouse world. Phil. Trans. R. Soc. Land. B 353, 29–39.
- 4 Woodward, F.I., Smith, T.M., Emanuel, W.R., 1995. A global land primary productivity and
5 phytogeography model. Global Biogeochem. Cycles 9, 471–490.
- 6 Wright, I.J., Reich, P.B., Westoby, M., Ackerly, D.D., Baruch, Z., Bongers, F., Cavender-Bares,
7 J., Chapin, T., Cornelissen, J.H.C., Diemer, M., Flexas, J., Garnier, E., Groom, P.K., Gulias, J.,
8 Hikosaka, K., Lamont, B.B., Lee, T., Lee, W., Lusk, C., Midgley, J.J., Navas, M., Niinemets,
9 U., Oleksyn, J., Osada, N., Poorter, H., Poot, P., Prior, L., Pyankov, V.I., Roumet, C., Thomas,
10 S.C., Tjoelker, M.G., Veneklaas, E.J., Villar, R., 2004. The worldwide leaf economics
11 spectrum. Nature 428, 821–827.
- 12 Yokota, T., Hagiwara, A., 1996. Seasonal change in the temperature coefficient Q₁₀ for
13 respiration of field-grown hinoki cypress (*Chamaecyparis obtusa*) trees. Journal of Forest
14 Research 1, 165–168.
- 15 Zeide, B., 2001. Natural thinning and environmental change: an ecological process model.
16 Forest Ecology and Management 154, 165–177.

Figures

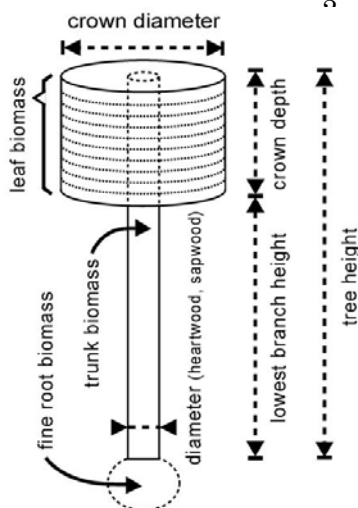


Figure 1

Representation of individual trees in the SEIB–DGVM. Each tree is composed of a crown, trunk, and fine roots. The trunk is composed of heartwood and sapwood. Trunk biomass includes branches and coarse/tap roots. The crown consists of 10-cm-deep ‘disks’. The trunk and the crown both have cylindrical shapes, while the fine roots are formless (i.e., represented only by biomass).

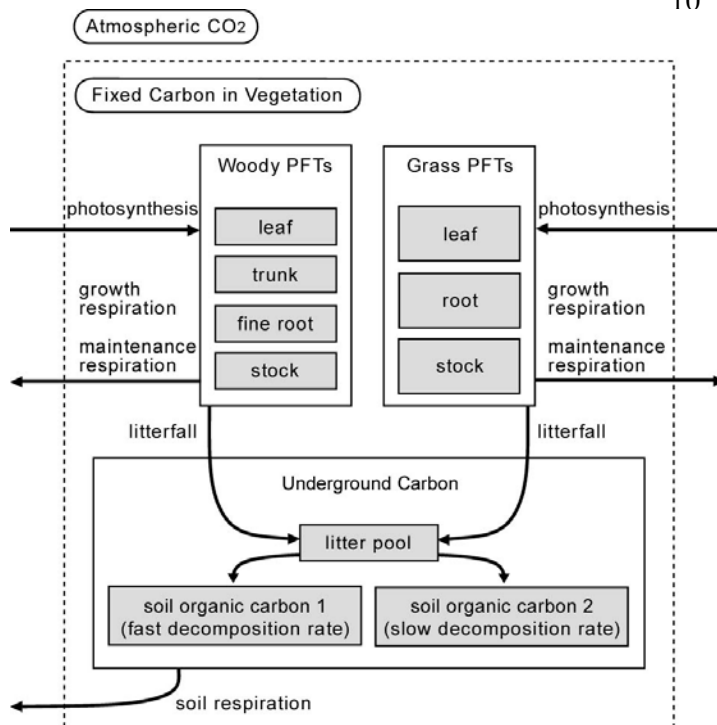


Figure 2

The carbon flow through a terrestrial ecosystem as simulated by the SEIB–DGVM.

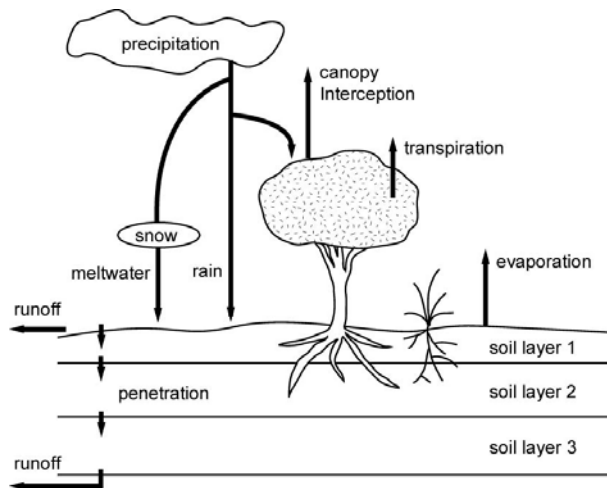


Figure 3

The water flow through the terrestrial ecosystem as simulated by the SEIB-DGVM.

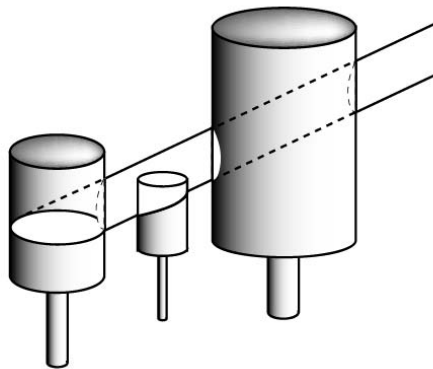


Figure 4

Schematic diagram of how to allocate direct radiation among trees in the SEIB-DGVM. See text for explanation.